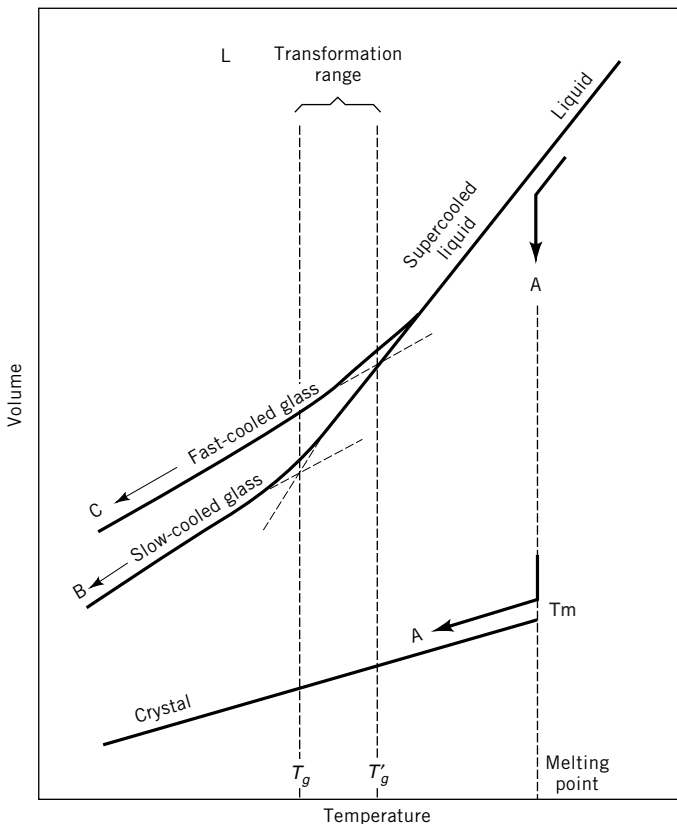


# GLASS

## 1. Introduction

Morey (1) defined glass as “an inorganic substance in a condition that is continuous with the liquid state, but which, as the result of a reversible change in viscosity during cooling, has attained so high a degree of viscosity as to be, for all practical purposes, rigid.” The American Society for Testing and Materials ASTM (2) defines glass as “an inorganic product of fusion that has been cooled to a rigid condition without crystallizing.” However, these definitions do not explicitly address the character of a noncrystalline structure and the glass-transformation behavior, two characteristics that separate glasses from other solids. In addition, glasses may be made by processes that do not necessarily produce liquids and so Shelby’s definition seems most appropriate: *Glass is a solid that possesses no long-range atomic order and, upon heating, gradually softens to the molten state* (3).

In principle, any melt forms a glass if cooled so rapidly that insufficient time is provided to allow reorganization of the structure into crystalline (periodic)



**Fig. 1.** Volume–temperature relationships for glasses, liquids, supercooled liquids, and crystals.

arrangements. When a liquid is cooled, its volume generally decreases until the melting point,  $T_m$ , is reached and then the volume changes abruptly as the liquid transforms into a crystalline solid (line A in Fig. 1. If a glass-forming liquid is cooled below  $T_m$  (line B) without the occurrence of crystallization, it is considered to be a supercooled liquid until the glass-transition temperature,  $T_g$ , is reached. (The  $T_g$  is the point below which the viscoelastic melt loses its liquid properties and the material behaves as a solid.) At temperatures below  $T_g$ , the material becomes a solid glass. Faster cooling leads to a greater  $T_g$  and a less dense glass (line C).

## 2. Fundamentals

**2.1. Kinetic Theory of Glass Formation.** Since most glasses are formed by quenching a melt from some temperature above the material's crystallization temperature down through the  $T_g$  and into the solid state, it is appropriate to discuss glass formation in terms of crystallization kinetics. That is, glass formation will occur if crystallization can be avoided when a melt is cooled, from  $T > T_m$  to  $T < T_g$ .

Classical nucleation and crystallization theory can be used to understand the conditions that promote glass formation (4). For a crystal nucleus to form, the atoms in a melt must reorganize to form an ordered crystal structure. In a supercooled melt at a temperature below the  $T_m$  of the crystal, crystalline solids are thermodynamically preferred over the disorganized melt. However, the surface energy,  $\gamma$ , required to create crystal nuclei is a thermodynamic barrier to the reorganization of the melt atoms into ordered structures, and the increasing melt viscosity,  $\eta$ , with decreasing temperature is a kinetic barrier. The dependence of the nucleation rate,  $I$ , on temperature,  $T$ , can be represented by

$$I = \frac{A}{\eta} \exp\left(\frac{B\gamma^3}{\Delta G_v T}\right) \quad (1)$$

where  $A$  and  $B$  are constants and  $\Delta G_v$  represents the free energy difference between the liquid and crystal. Crystals will form from stable nuclei in melts below  $T_m$  at a rate ( $U$ ) given by

$$U = \frac{CT}{\eta} \left[ 1 - \exp\left(\frac{\Delta G_v}{kT}\right) \right] \quad (2)$$

where  $C$  is a constant and  $k$  is Boltzmann's constant.

A schematic representation of the temperature dependences of nucleation and crystallization rates described by equations (1) and (2) is shown in Figure 2. For glass formation to occur, a melt must be quenched from a temperature above  $T_m$  to below  $T_g$  while avoiding significant (detectable) crystallization. The increase in melt viscosity as the melt is cooled below  $T_m$  counters the free energy gained by crystallization so that nucleation and crystal growth are no longer kinetically significant at temperatures below the  $T_g$ . As a result, materials like  $\text{SiO}_2$  that possess high viscosities ( $\sim 10^6$  Pa·s) at  $T_m$  are easily quenched to

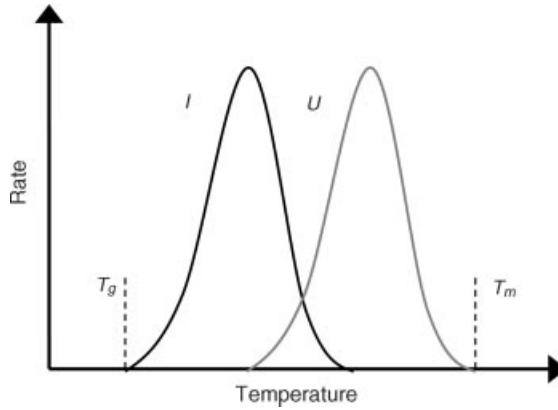


**Fig. 2.** Schematic representation of the classical rates for nucleation  $I$ , and crystallization,  $U$ , for a supercooled melt between the melting point,  $T_m$  and the glass-transition temperature,  $T_g$ .

form glasses, whereas materials like water that possess low viscosities ( $\sim 10^{-3}$  Pa·s) at  $T_m$  form glasses only under extreme conditions.

Time–temperature transformation (TTT) diagrams (Fig. 3) are another way to represent the relationships between quenching rates and glass formation. Crystal growth kinetics can be used to predict the times and temperatures necessary to convert some fraction of a supercooled melt to crystallized material. Curve A in Figure 3 represents a material with a low viscosity at  $T_m$  and curve B represents a material with a high viscosity at  $T_m$ . The latter material will require longer times at a fixed temperature to acquire the same level of crystallization. To avoid the levels of crystallization represented by the curves, the two melts must be quenched at rates faster than those represented by the dashed lines between  $T_m$  and the respective “nose temperatures” of the crystallization curves. The high viscosity melt represented by line B will require a lower critical

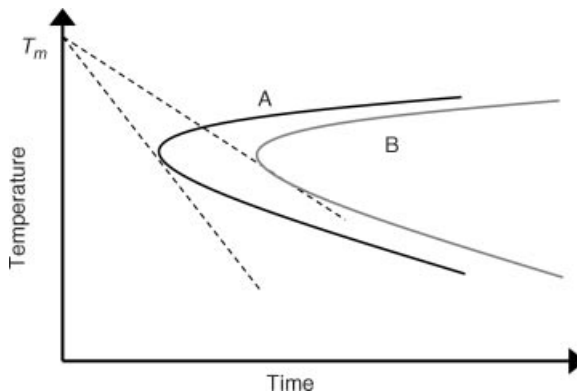


**Fig. 3.** Time–temperature transformation curves representing supercooled melts with low (curve A) and high viscosities (curve B) at  $T_m$ . The dashed lines represent the critical cooling rates to avoid crystallization.

quenching rate to avoid crystallization, and so will be classified as a better glass-forming material.

To summarize, glass formation will occur when a melt is quenched to temperatures below the  $T_g$  at a rapid enough rate to avoid detectable crystallization. Melts with high viscosities at the crystal melting temperature (or melts that exhibit rapid viscosity increases when cooled below  $T_m$ ) are most easily quenched

Table 1. Main Inorganic Glass Systems<sup>a</sup>

One element	B, C, P, As, S, Se		
group 16 (VIA) chalcogenides <sup>b</sup>	oxides	glass formers	P <sub>2</sub> O <sub>5</sub> , As <sub>2</sub> O <sub>5</sub> , SiO <sub>2</sub> , GeO <sub>2</sub> , B <sub>2</sub> O <sub>3</sub>
		intermediate formers	MoO <sub>3</sub> , WO <sub>3</sub> , TiO <sub>2</sub> , Fe <sub>2</sub> O <sub>3</sub> , Al <sub>2</sub> O <sub>3</sub> , Ga <sub>2</sub> O <sub>3</sub> , Bi <sub>2</sub> O <sub>3</sub> , BeO, PbO, Nb <sub>2</sub> O <sub>5</sub> , Ta <sub>2</sub> O <sub>5</sub>
	sulfides	glass formers	As <sub>2</sub> S <sub>5</sub> , SiS <sub>2</sub> , GeS <sub>2</sub> , B <sub>2</sub> S <sub>3</sub> , Al <sub>2</sub> S <sub>3</sub> , Ge <sub>2</sub> S <sub>3</sub> , As <sub>2</sub> S <sub>3</sub> , Sb <sub>2</sub> S <sub>3</sub>
		intermediate formers	P <sub>2</sub> S <sub>5</sub> , Ga <sub>2</sub> S <sub>3</sub> , In <sub>2</sub> S <sub>3</sub>
	tellurides	GeTe <sub>2</sub> , Si <sub>2</sub> Te <sub>3</sub> , GaTe, GeTe, SnTe, As <sub>2</sub> Te <sub>3</sub>	
three-element chalcogenide systems	Ge-As-S, Ge-As-Se, Ge-As-Te, Ge-Sb-Se, As-Sb-Se, As-S-Se, As-S-Te, As-Se-Te, S-Se-Te		
group 17 (VIIA) halides	fluorides	glass formers	BeF <sub>2</sub>
		intermediate formers	ZrF <sub>4</sub> , HfF <sub>4</sub> , ThF <sub>4</sub> , UF <sub>4</sub> , ScF <sub>3</sub> , YF <sub>3</sub> , CrF <sub>3</sub> , FeF <sub>3</sub> , AlF <sub>3</sub> , GaF <sub>3</sub> , InF <sub>3</sub> , ZnF <sub>2</sub> , CdF <sub>2</sub> , PbF <sub>2</sub>
	chlorides	glass formers	ZnCl <sub>2</sub>
		intermediate formers	ThCl <sub>4</sub> , BiCl <sub>3</sub> , CdCl <sub>2</sub> , SnCl <sub>2</sub> , PbCl <sub>2</sub> , CuCl, AgCl, TlCl
	bromides	glass formers intermediate formers	ZnBr <sub>2</sub> PbBr <sub>2</sub> , CuBr, AgBr
iodides	glass formers intermediate formers	ZnI <sub>2</sub> CdI <sub>2</sub> , PbI <sub>2</sub> , CuI, AgI	
complex glasses and nonsilicate glasses	oxyhalides, chalcahalides (Se-Te-X; XCl, Br, I), oxyfluorophosphates, oxynitrides (ie, SiAlON glasses), carbonates, nitrates, nitrites, sulfates, selenates, alkali dichromates		

<sup>a</sup>adapted from Ref. 5.

<sup>b</sup>Chalcogen(ide) refers to any of the elements oxygen, sulfur, selenium, and tellurium. However, oxide-based glasses have far more commercial and technological importance today than any other chalcogenide-based glass. See also the section on Chalcogenide Glasses.

to form glasses. Certain materials possess lower critical cooling rates and so more readily form glasses. These glass-forming materials are described in subsequent sections.

**2.2. Structural Descriptions of Glass-Forming Systems.** Inorganic glasses are readily formed from a wide variety of materials, principally oxides, chalcogenides, halides, salts, and combinations of each. Table 1 summarizes the more common inorganic glass systems.

There have been many attempts to relate the glass-forming tendency of a material to its molecular level structure. For example, Goldschmidt (6) observed that oxide glasses with the general formula  $R_nO_m$  form most easily when the ionic radius ratio of the metal cation and the oxygen ion lies in the range between 0.2 and 0.4. Zachariasen (7) noted that those crystalline oxides that form open, continuous networks tended to form glasses and those glass-forming networks were associated with ions with particular coordination numbers (CN). Zachariasen proposed that the structure of glass was similar to that of a crystal, but with a larger lattice energy resulting from the disordered arrangements of polyhedral units, to possess a random network lacking long-range periodicity, as shown schematically in Figure 4 (7). Zachariasen listed four conditions for a structure to favor glass formation: (1) an oxygen or anion must not be linked to more than two cations; (2) the number of oxygens or anions coordinated to the cations must be small, typically three or four; and (3) the cation–anion polyhedra must share corners rather than edges or faces; (4) at least three corners must be shared. These conditions lead to the open structures that can accommodate a distribution of interpolyhedral bond angles that are associated with the loss of long-range structural order when a crystal form a glass. Subsequent diffraction studies by Warren (8) and others (ie, Ref. 9) confirmed Zachariasen's prediction that glasses

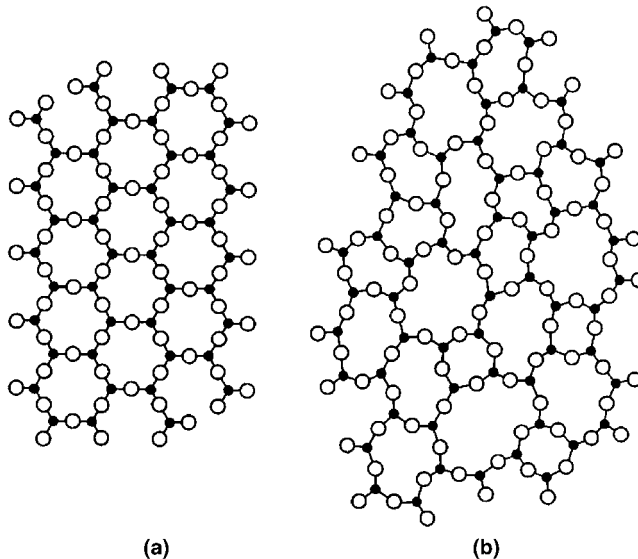


**Fig. 4.** Schematic two-dimensional (2D) representation of the silica random network built by  $\text{SiO}_4$  tetrahedra: (a) crystalline structure (or long-range order), (b) random network (7).

and crystals possess similar short-range polyhedral structures but different long-range polyhedral arrangements.

Oxides that do not possess the open network structures of the glass-forming oxides are sometimes classified as network modifiers or intermediate oxides, depending on their structural roles (Table 2). Oxides with large coordination numbers and relatively weak bonds are called network modifiers and they alter the glass-forming network by replacing stronger bridging oxygen (BO) bonds between glass-forming polyhedra with weaker, nonbridging oxygen

Table 2. Bond Strengths and Coordination Number of Oxides of Technological Significance<sup>a</sup>

Oxide	Dissociation energy, kJ/mol	Coordination number	Single-bond strength, kJ/mol	CAS Registry number
<i>Glass former</i>				
B <sub>2</sub> O <sub>3</sub>	1489	3; 4	496; 372	[1303-86-2]
SiO <sub>2</sub>	1774	4	443	[10097-28-6]
GeO <sub>2</sub>	1803	4	450	[1310-53-8]
P <sub>2</sub> O <sub>5</sub>	1849	4	462–370	[1314-56-3]
V <sub>2</sub> O <sub>5</sub>	1879	4	469–376	[1314-62-1]
As <sub>2</sub> O <sub>5</sub>	1460	4	365–292	[1303-28-2]
Sb <sub>2</sub> O <sub>5</sub>	1418	4	354–284	[1314-60-9]
<i>Intermediates</i>				
TiO <sub>2</sub>	1820	6	303	[13463-67-7]
ZnO	602	2	301	[1314-13-2]
PbO	606	2	303	[1317-36-8]
Al <sub>2</sub> O <sub>3</sub>	1682-1326	4; 6	420–332; 280–221	[1344-28-1]
ThO <sub>2</sub>	2159	8	269	[1314-20-1]
BeO	1046	4	261	[1304-56-9]
ZrO <sub>2</sub>	2029	6; 8	338; 253	[1314-23-4]
CdO	498	6	248	[1306-19-0]
<i>Modifiers</i>				
Sc <sub>2</sub> O <sub>3</sub>	1514	6	252	[12060-08-1]
La <sub>2</sub> O <sub>3</sub>	1699	7	242	[1312-81-8]
Y <sub>2</sub> O <sub>3</sub>	1669	8	208	[1314-36-9]
SnO <sub>2</sub>	1163	6	193	[18282-10-5]
ThO <sub>2</sub>	2159	12	179	[1314-20-1]
PbO <sub>2</sub>	970	6	161	[1309-60-0]
MgO	929	6	154	[1309-48-4]
Li <sub>2</sub> O	602	4	150	[12057-24-8]
PbO	606	4	151	[1317-36-8]
ZnO	602	4	150	[1314-13-2]
BaO	1088	8	135	[1304-28-5]
CaO	1075	8	134	[1305-78-8]
SrO	1071	8	133	[1314-11-0]
CdO	498	4; 6	124; 82	[1306-19-0]
Na <sub>2</sub> O	502	6	83	[1313-59-3]
K <sub>2</sub> O	491	9	53	[12136-45-7]
Rb <sub>2</sub> O	481	10	48	[18088-53-2]
Cs <sub>2</sub> O	447	12	39	[20281-00-9]

<sup>a</sup>Ref. 10

(NBO) bonds to modifying polyhedra (Fig. 5). The network modifiers are important constituents to most technological glasses because they lower the melting temperature and control many useful properties. The intermediate oxides have coordination numbers and bond strengths between the network formers and network modifiers and tend to have an intermediate effect on glass properties.

**Silicate Glasses.** The structure of silica glass consists of well-defined  $\text{SiO}_4$  tetrahedra connected to another neighboring tetrahedron through each corner. Neutron diffraction studies indicate that the Si–O distance in the tetrahedron is 0.161 nm and that the shortest O–O distance is 0.263 nm, the same dimensions as found in crystalline silica (9). The intertetrahedral (Si–O–Si) bond angle distribution is centered near  $\sim 143^\circ$ , but is much broader than that found for crystalline silica, producing the loss in long-range order shown schematically in Figure 4.

The structure of alkali silicate glasses also consists of a network of  $\text{SiO}_4$  tetrahedra, but some of the corners are now occupied by non-bridging oxygens that are linked to the modifying polyhedra (Fig. 5). Increasing the concentration of modifying oxide ( $\text{R}_2\text{O}$ ) increases the relative fraction of nonbridging oxygens associated with the glass network and so reduces the  $T_g$  and melt viscosity

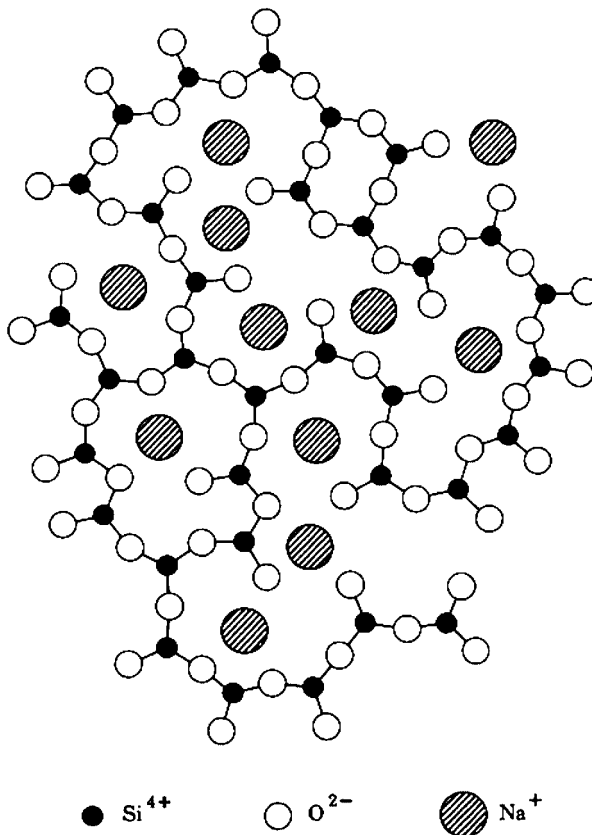


**Fig. 5.** Schematic 2D representation of the random network of alkali silicates (11).

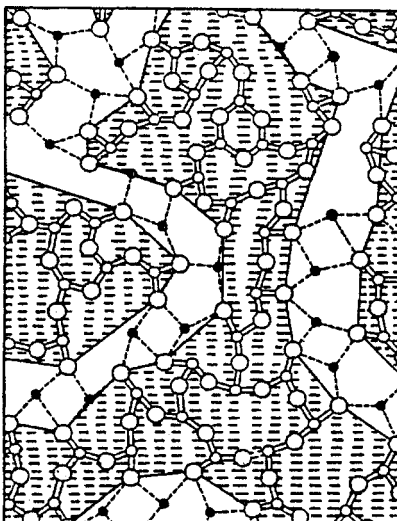


**Fig. 6.** Modified random structure showing “alkali channels” (14).

and increase thermal expansion coefficient and ionic conductivity. The changes in the silicate network, and so the compositional dependence of many of the glass properties, can be described by the relative fractions of bridging and nonbridging oxygens or by the types and concentrations of the different Si-tetrahedra, viz, tetrahedra that possess four bridging oxygens (sometimes called  $Q^4$  tetrahedra), those with three BOs ( $Q^3$ ), etc. On the atomic scale (0.1–5 nm), the distributions of modifying alkali ions ( $R^+$ ) around bridging oxygens and nonbridging oxygens, as well as the  $R$ – $R$  distributions are not random (12,13). One view of the glass structure is a “modified random network” in which the alkali ions and NBO cluster to form alkali-rich regions surrounded by presilicate network (Fig. 6). X-ray and neutron diffraction studies, extended X-ray absorption fine structure (EXAFS) data (14,15), and molecular dynamics (MD) simulations (16) give a picture of the glass structure consistent with that shown in Figure 6 (14).

Glasses containing < 10 mol% alkali oxides are considerably more difficult to melt due to higher viscosities (17). Alkali-deficient glasses are prone to phase separation and devitrification on a scale of 0.1–1  $\mu\text{m}$  (18).

**Borate Glasses.** There are several reviews on the network structure of borate glasses and alkali borate glasses (19–25). The structure of vitreous  $\text{B}_2\text{O}_3$  consists of planar triangular  $\text{BO}_3$  units that link to form larger units known as boroxol rings (see Figure 7). These well-defined units are connected by oxygens so that the B–O–B angle is variable and twisting out of the plane of the boroxol group can occur, producing the loss of long range order associated with glass. For vitreous boron trioxide (v- $\text{B}_2\text{O}_3$ ) the results by MD and quantum mechanical simulations (21,26), nuclear magnetic resonance (nmr) (22), nuclear quantum resonance (nqr) (23), ir and Raman spectroscopic (24) studies, and inelastic neutron scattering (25) all indicate that a large fraction of B atoms ( $\sim 80$ – $85\%$ ) are in the planar boroxol rings.

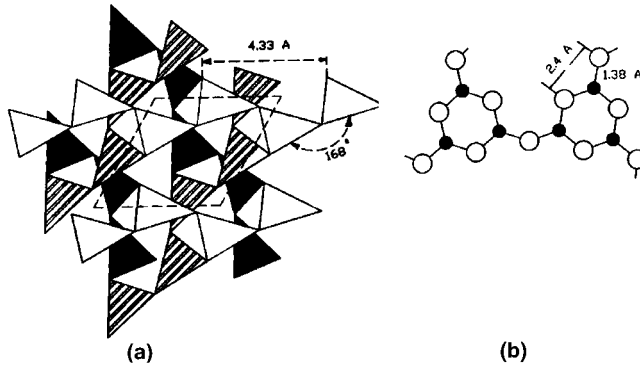


**Fig. 7.** (a) Structure of crystalline  $B_2O_3$  formed by  $BO_3$  triangles and (b) boroxol unit (20).

When an alkali oxide is first added to  $B_2O_3$ , the  $T_g$  increases and the coefficient of thermal expansion (CTE) decreases, and property trends are opposite to those observed when modifying oxides are added to silica. This behavior is sometimes called the “Borate Anomaly” and it can be explained by the compositionally dependent changes in the borate glass structure. For glasses with the molar composition  $xR_2O \cdot (1-x)B_2O_3$ , the initial addition (up to  $x \sim 0.25$ ) of an alkali oxide to  $B_2O_3$  causes the trigonal borons ( $B_3$ ) associated with boroxol rings and “loose”  $BO_3$  triangles to convert to tetrahedral borons ( $B_4$ ) (27). Each of the four oxygens associated with these new tetrahedral sites are bridging oxygens, and so the changes in glass properties that define the borate anomaly can be explained by the increasing number of structural linkages (through bridging B–O–B bonds) with the initial addition of the modifying oxide. A maximum concentration of  $B_4$  sites are present when  $x \sim 0.30$  and further additions of the modifying oxide leads to the replacement of the  $B_4$  units with  $B_3$  units that possess nonbridging oxygens (23,28). As a consequence,  $T_g$  decreases and thermal expansion coefficient increases with additions of  $R_2O$  beyond  $\sim 30$  mol%.

**Phosphate Glasses.** The basic building blocks of crystalline and amorphous phosphates are  $PO_4$ -tetrahedra. These tetrahedra link through covalent bridging oxygens to form various phosphate anions (see Fig. 8). The tetrahedra

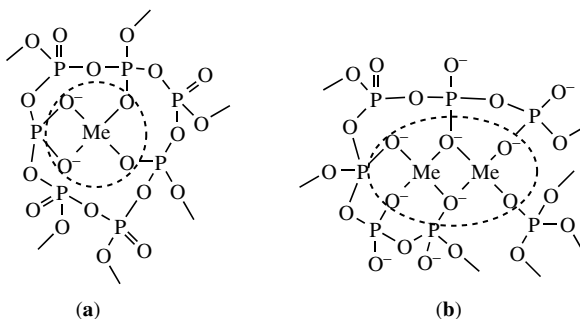
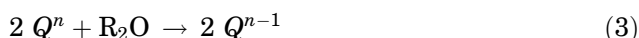


**Fig. 8.** Ultraphosphate glass structure in different concentrations of modifier ions (Me), terminal oxygens  $>$  modifier ions (a) and terminal oxygens  $<$  modifier ions (b) (30).

are classified using the  $Q^n$  terminology (29), mentioned above, where  $n$  represents the number of bridging oxygens per tetrahedron. The networks of phosphate glasses can be classified by the oxygen/phosphorus ratio, which sets the number of linkages through bridging oxygens to neighboring P-tetrahedra. Thus, metaphosphate ( $O/P = 3$ ) and polyphosphate ( $O/P > 3$ ) glasses have structures that are based on chain-like phosphate anions that are themselves interconnected through terminal oxygens by ionic bonds with modifying cations (30) and ultraphosphate ( $O/P < 3$ ) glasses have network that are cross-linked by  $Q^3$  tetrahedral with three BO and one double-bonded nonbridging oxygen to satisfy the +5 valence of the phosphorus (31).

The addition of an alkali or alkaline earth oxide to  $P_2O_5$  depolymerizes the three-dimensional (3D)  $Q^3$  network to form the chain-like  $Q^2$  sites. The resulting depolymerization of the phosphate network with the addition of alkali oxide,  $R_2O$ , is described by the pseudo-reaction (32)



The extent of the network polymerization in silicate and phosphate glasses changes monotonically as a function of composition, however, the compositional dependence of a variety of ultraphosphate glass properties, are anomalous when compared with the silicate analogues (33,34). For example, the minimum in density at  $\sim 20$  mol%  $Na_2O$  (Fig. 9) is not consistent with simple network depolymerization and alkali packing (30,35).

In diffraction studies of binary ultraphosphate glasses, Hoppe and co-workers (36) described the role that the modifier coordination plays in determining the properties and structures of phosphates glasses. Hoppe assumed that only nonbridging oxygens participate in the coordination shell of the modifier cations. At low concentrations of modifier oxide, sufficient numbers of nonbridging oxygens are available to isolate the individual modifier polyhedra (Fig. 8(a)) but a higher concentrations, the increasing numbers of modifying polyhedra must share available NBOs (Fig. 8(b)). The composition at which this change in modifier packing occurs is dependent on the modifier coordination number and

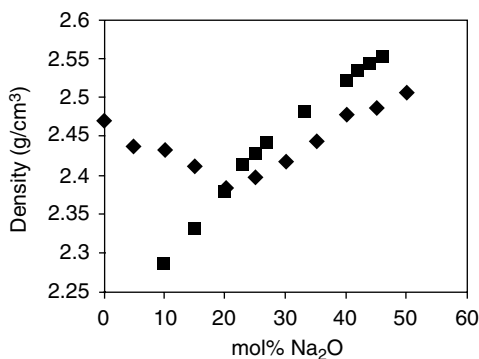


**Fig. 9.** Density of sodium ultraphosphate glasses (30). ◆ Na-phosphates ■ Na-silicates

can be related to the changes in glass properties. Thus, the phosphates are an example of a glass-forming system in which a detailed understanding of the structural roles played by both the glass forming and modifying constituents must be obtained to properly explain composition–property relationships.

**Germanate Glasses.** The structure of  $\text{GeO}_2$  glass is very similar to that of  $\text{SiO}_2$  glass, with basic building block of germanium–oxygen  $Q^4$  units (37). Since the  $\text{Ge}^{4+}$  ion is larger in diameter than the  $\text{Si}^{4+}$  ion, the Ge–O distance is also larger than the Si–O distance (in silicate glasses), with a bond length of  $\sim 0.173$  nm and Ge–O–Ge bond angle smaller than the Si–O–Si bond angle. Gas diffusion studies suggest that the open volume of germanate glass is slightly less than that of silicate glass (38). Recent reports including neutron diffraction (39), high energy photon diffraction (using synchrotron radiation) (40), magic angle spinning nuclear resonance (mas nmr) (41) and Raman spectroscopy (42), suggest that the structure of vitreous germania resembles that of quartz-like  $\text{GeO}_2$ , with  $[\text{GeO}_4]$  tetrahedra providing the basic structural units, giving a continuous random network. Jain and co-workers (43) have used xps (x-ray photoelectron spectroscopy) to investigate the effect of alkali additions to germania, showing, in contrast to previous models, that nonbridging oxygens are formed at very low alkali concentrations ( $\sim 2\%$ ) along with  $\text{GeO}_6$  units.

**Chalcogenide Glasses.** Chalcogenide glasses are produced by melting group 16 (VI A) elements (S, Se, and Te) with other elements, generally of group 15 (V A) (eg, Sb, As) and group 14 (IV A) (eg, Ge, Si) to form covalently bonded solids. When melted in an atmosphere particularly deficient in oxygen and water, the glasses have unique optical and semiconducting properties (44). Structural models for these glasses are based on the high degree of covalent bonding between chalcogenide atoms. Since the chalcogenide glasses are a set of continuously varying compositions of elements having a varying covalent coordination number, it is generally useful to invoke the concept of the atom-averaged covalent coordination,  $\langle r \rangle$ , as a structural attribute

$$\langle r \rangle = \sum r_i a_i \quad (i = 1, 2, \dots, n), \quad (4)$$

where  $r_i$  is the covalent coordination number of element  $i$  having atom fraction  $a_i$  in the glass. Thorpe (45) suggested that glasses having  $\langle r \rangle < 2.4$  possess structures with regions whose volume fractions are too small to be fully connected. This lack of full connectivity results in a “polymeric” solid where the rigid regions are surrounded by a “floppy” matrix. When,  $\langle r \rangle > 2.4$ , the solid has continuously connected rigid regions with floppy regions interdispersed and may be termed an “amorphous solid”. The  $\langle r \rangle = 2.4$  glass is unique in that it has the number of constraints equal to the number of degrees of freedom, consisting of floppy and rigid regions individually connected by matrices with maximum number of connections. There are a number of studies that relate the degree of structural connectivity to the glass-forming tendency and properties of chalcogenide glasses eg. (46–48).

**Halide Glasses.** Structural models for fluoride glasses based on  $\text{BeF}_2$  are directly analogous to those for alkali silicate glasses, with the replacement of nonbridging oxygens by nonbridging fluorines (NBF). Fluoride glasses have been studied for the past 30 years and have found various applications in optics

(48), sensors (49), is instrumentation, medicine and telecommunications (50). Of particular importance are the heavy metal fluoride glasses (HMFG) based on  $ZrF_4$  in numerous multicomponent systems in which some fluorides act as glass formers in association with alkali and divalent fluorides (51). Extensive development work has also been carried out on fluorophosphate glass (5–20%  $P_2O_5$ ), initially for use as optical glasses but more recently for use in high power lasers (52).

**Organic Glasses.** Organic glasses consist of carbon–carbon chains, which are so entangled, that rapid cooling of the melt prevents reorientation into crystalline regions. Like low crystallinity glass–ceramics, the organic glasses presented small regions of oriented chains (53). Low molecular weight organic glasses are increasingly investigated because they potentially combine several interesting properties such as easy purification, good processability and high gas solubility (54). Numerous applications are envisaged, eg, in light emitting devices (55), in nonlinear optics (56), in optical data storage (57), and in photovoltaic and photochromic materials (58). Consequently, the influence of the molecular structure on stability of the glass and on the  $T_g$  is an important question.

**Metallic Glasses.** Structural models for metallic glasses include variations of the random network theory, crystalline theory, and a dense random packing of spheres. Structural methods such as X-ray diffraction (59), electron microscopy (60), Mössbauer resonance, nmr, and thermal analysis (61), have been used to study the structures of glassy metals. Heat capacity data demonstrated that the metals were indeed vitreous and not amorphous with microcrystallization.

Metallic glasses were first produced commercially as ribbons or fibers 50–100  $\mu\text{m}$  thick and up to 25 mm wide. For example, bulk glassy alloys in the Mg (62), La- and Zr- (63) based system, having a large supercooled liquid region before crystallization, have attracted much interest as new materials in science and engineering fields (64). The glass-formation ability of a melt is evaluated in terms of the critical cooling rate,  $R_c$ , for glass formation. The critical cooling rate is the minimum cooling rate necessary to keep the melt amorphous without precipitation of crystals during the solidification and is shown schematically in Figure 3. There are now some compositions, with lower  $R_c$ , that can be cast as monoliths. For example, metallic glasses such as  $Au_{77.8}Si_{8.4}Ge_{13.8}$  and  $Fe_{91}B_9$  have  $R_c$  of  $3 \times 10^6$  and  $2.6 \times 10^7$  K/s (60), respectively, whereas more recent bulk metallic glasses based on alloys of Zr, Ti, Cu, Ni, and Be have critical cooling rates on the order of 10 K/s (65,66).

Many studies on the formation and structure (ie, Refs. 67–69), physical and mechanical properties, and  $T_g$  and crystallization process of glassy alloys have been reported (ie, Refs. 70,71). Examples include Fe-based bulk metallic glasses, which have been prepared in Fe–(Al, Ga)–(P, C, B, Si) (72), Fe–(Co,Ni)–(Zn, Nb, Ta)(73), and Fe–C–Si–B, Fe–Ni–P–B system (74). They exhibit high glass-forming ability, good mechanical properties, and soft magnetic properties. However, there are few results about corrosion resistance of iron-based bulk glassy.

**2.3. Computer Modeling of the Glass Structure.** Recent software and hardware developments have produced a new characterization technique for glass structure: atomistic simulations based on MD calculations of silicates

(75,76), borate glasses (77,78), and phosphate glasses (79). Static lattice simulations cannot be applied in a straightforward way to glasses as in the study of physics and chemistry of crystalline solids. The MD studies of alkali silicates (Na-, K-, Na-K, and Li) provide “snapshot” pictures of the atomic configuration. This allows the identification of key features and correlation of the atomic scale structure with the macroscopic experimental properties.

The distribution of alkali modifiers throughout the glass network is one aspect of technological importance. Studies of alkali silicate glasses reveal that the alkali ions are not randomly distributed within the silica network but rather aggregate in alkali-rich regions on a nanoscale, consistent with the “modified random network” structural model introduced in the section on Silicate Glasses (75). Lithium-silicates exhibit the greatest degree of aggregation, possibly because of the size and mobility of the ion. The disilicate composition marks the onset of the thermodynamically predicted homogeneous glass-forming region. Such results help relate phase separation and immiscibility tendencies for the alkali silicates to structural and thermodynamic considerations.

Surfaces can be modeled using MD in two ways (77): by removing the periodicity in one dimension or by increasing the dimension of one of the box edges, without scaling the atomic coordinates. The second method creates a series of 2D slabs with top and bottom surfaces. Figure 10 shows the vitreous silica surface computer simulations obtained at the New York State College of Ceramics at Alfred University. Such calculations give new insight on the glass structure. Direct views of the structure of a silica glass fracture surface and comparison with a structure calculated by MD simulation of  $\text{SiO}_2$  glass surface provides support for Zachariassen’s random network structure model of glass (80).

**2.4. Glass Ceramics.** Glass-ceramics are normally obtained by a controlled crystallization process of suitable glass-forming melts. Internal or external nucleation is promoted to develop microheterogeneities from which crystallization can subsequently begin. As a result, the amorphous matrix transforms into a microcrystalline ceramic aggregate. The composition of the

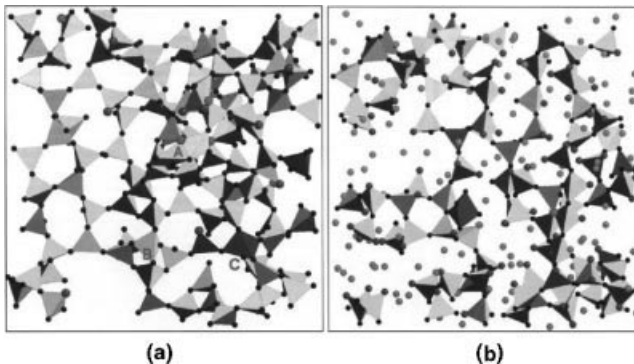


**Fig. 10.** (a) Top view of vitreous silica surface with an area of  $2.83 \times 2.83 \text{ nm}^2$ . All species  $>2.9 \text{ nm}$  are shown: threefold Si (turquoise triangle), fourfold Si (yellow polyhedron), fivefold Si (purple polyhedron), NBO (purple sphere), BO (blue sphere), and TBO (terminal BO, red sphere); (b) Top view of 30% sodium silicate glass surface with an area of  $2.732 \times 2.732 \text{ nm}^2$ , showing all species  $>2.7 \text{ nm}$  (75).

crystalline phases and the crystalline sizes define the properties of the final material. Therefore, the major components and the composition of the glass are selected to ensure precipitation of crystals that provide desired properties of the glass–ceramic (81–83). By definition, glass–ceramics are  $> 50\%$  crystalline after heat treatment; frequently, the final product is  $> 90\%$  crystalline. In general, the heat treatment necessary to convert the base glass into a glass ceramic increases the fabrication costs of a component. Consequently, many interesting glass ceramics have been developed, but not all of them have been commercially successful, due to the ratio between customer benefit and unattractive price (84).

Aluminosilicate glass–ceramics are among the most useful commercial products. The addition of nucleation agents such as  $\text{TiO}_2$  or  $\text{TiO}_2 + \text{ZrO}_2$  and the selection of the optimum heat treatment schedule controls the distribution and morphology of the final crystal structures. Many other components can be added to optimize the crystalline phases and the glass–ceramic properties. Certain lithium aluminosilicates have low expansion and good chemical durability. Sodium aluminosilicates and barium–sodium aluminosilicates have high expansion and can be strengthened by surface compression techniques such as the application of a low expansion glaze. Magnesium aluminosilicates have low expansion and can have very high strength. Fluorine added to potassium–magnesium aluminosilicate increases machinability (85).

Other systems preferentially crystallize at surfaces, thus glass powders can be converted to glass–ceramics without the need for the addition of special nucleating agents. The densification of the glass–powder compact must take place prior to crystallization. During the sintering stage, the glass grains first densify by viscous flow and then nucleate at and crystallize from the original glass–particle boundaries. Surface nucleation is very important for many applications of sintered glass–ceramics and in most cases, surface crystallization is delayed until densification has proceeded. Table 3 shows examples of commercial glass–ceramic systems.

**2.5. Devitrification and Phase Separation.** Devitrification is the uncontrolled formation of crystals in glass during melting, forming, or secondary processing in contrast to the controlled crystallization associated with glass–ceramic processing. Devitrification can affect glass properties including optical transparency, mechanical strength, and sometimes the chemical durability. As discussed in the section Kinetic Theory of Glass formation, glass-formation ability (GFA) depends on the avoidance of devitrification. The GFA of a melt is evaluated in terms of the critical cooling rate  $R_c$ , for glass formation, which is defined as the minimum cooling rate necessary avoid precipitation of any detectable crystals during solidification. Systems with lower  $R_c$  (line B in Fig. 3) have greater GFA. The supercooled liquid temperature  $\Delta T_{xg}$  (the temperature difference between the onset crystallization temperature  $T_x$  and the  $T_g$ ), is another indication of the devitrification tendency of a glass upon heating above  $T_g$ . A large  $\Delta T_{xg}$  value indicates that the supercooled liquid can exist in a wide temperature range without crystallization and has a high resistance to devitrification (87).

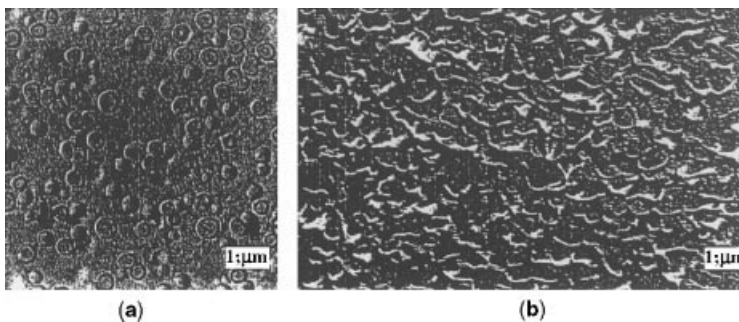
Glasses that derive their color, optical transparency, or chemical durability from a small amount of a finely dispersed, amorphous, second phase are termed phase-separated glass, distinguished from glass ceramics because they remain predominantly amorphous. Phase separation can occur by processes: (1) nuclea-

Table 3. Commercial Glass–Ceramics<sup>a</sup>

Commercial designation	Major crystalline phases	Properties	Application
Corning 9632	$\beta$ -quartz solid [14808-60-7]	low expansion, high strength, thermal stability	electrical range tops
Corning 9608	$\beta$ -spodumene solid solution, $\text{Li}_2\text{O} \cdot \text{Al}_2\text{O}_3 \cdot (\text{SiO}_2)_4$	low expansion, high chemical durability	cooking utensils
Neoceram (Japan)	$\beta$ -spodumene [1302-37-0]	low expansion	cooking ware
Corning 0303	nepheline [12251-37-3], $\text{Na}_2\text{O} \cdot \text{Al}_2\text{O}_3 \cdot 2\text{SiO}_2$	high strength, bright white	tableware
Corning 9625	$\alpha$ -quartz solid solution ( $\text{SiO}_2$ ); spinel ( $\text{MgO} \cdot \text{Al}_2\text{O}_3$ ); enstatite $\text{MgO} \cdot \text{SiO}_2$	very high strength	classified
High K (Corning)	$3\text{Al}_2\text{O}_3 \cdot 2\text{SiO}_2$ ; (Ba, Sr, Pb) $\text{Nb}_2\text{O}_6$	high dielectric constant	capacitors
Corning 9455	$\beta$ -spodumene solid solution; mullite [1302-93-8], $3\text{Al}_2\text{O}_3 \cdot 2\text{SiO}_2$	low expansion, high thermal and mechanical stability	heat exchangers

<sup>a</sup>Ref. 86.

tion and growth and (2) spinodal decomposition (88). The morphologies of the phase-separation microstructures obtained by these two different processes are different. Spinodal decomposition produces a composite material with two highly interconnected amorphous phases, whereas phase separation that occurs by the classical nucleation process produces a microstructure in which discrete, spherical droplets are embedded in an amorphous matrix (89). The most important parameter affecting the morphology of phase separation is the composition of the liquid. Discrete particle morphologies will be observed for compositions near the edges of liquid–liquid miscibility gaps. Morphologies with larger volume fractions of both phases, often with a greater degree of connectivity, will be found for composition near the center of miscibility gaps. Figure 11 summarizes and exemplifies nucleated phase separation and spinodal decomposition.



**Fig. 11.** Microstructural morphology of immiscibility in glasses: (a) sodium-borosilicate glass showing a nucleated type of phase separation, and (b) sodium-borosilicate glass composition from center of immiscibility region (spinodal decomposition) (90).

**2.6. Surfaces of Glasses.** The surface of a glass plays a major role in its ability to function in a given application. For example, optical applications may require smooth glass surfaces to precise dimensions (ie, lenses) and high chemical durability. In other applications, the surface must form appropriate bonds to specific materials (decorations, coatings). Four characteristics of the surface make a glass suitable for particular applications: (1) ability to be ground and polished, (2) chemical durability, (3) ability to bond specific molecules, and (4) resistance to mechanical damage (strength is limited by presence of Griffith flaws). Table 4 summarizes selected tools and techniques for the study of glass surfaces (91,92).

Fiber surface characteristics determine most of the important properties of continuous glass fibers used for composite reinforcements. Applications of coatings (sizing) agents serve many purposes, including process compatibility, scratch protection, chemical passivation, and adhesion promotion.

The use of glass as a substrate for flat-panel displays (FPD) exerts considerable demands on the glass surface. It must be smooth, free of particulate contamination and capable of interfacing with metals, semiconductors, oxides, and polymers. In the manufacture of FPD devices, the surface must withstand the chemical and physical processes associated with wet and dry cleaning, chemical etching, polishing, and plasma treatments.

### 3. Properties

The properties of glasses depend on their chemical composition and their structure. Most properties can be discussed from a starting point represented by the material of the crystalline form by considering what modifications, structural disorder, absence of translation periodicity, spatial variations in atomic concentrations or local structure will have on the chosen property (93). A major advantage of glasses is that their properties can be tailored by adjusting their composition. As a first approximation, a final given property can be expressed as a simple additive function of its relative oxide contents. However, in some cases the relationship is more complex (ie, borate anomaly). Several compilations of experimental results are useful sources of data (94,95). More recently, such compilations are maintained electronically. For example, *Sciglass* (96) is a database that includes >1,000,000 experimental values for 105,000 glasses, >60% of the world's published glass data. *Interglad* (International Glass Database System) is another commercial electronic system compiling data on >190,000 glasses of different compositions (97).

Another compilation is being generated by the National Science Foundation (NSF)–Industry University Center for Glass Research (CGR), where researchers at Alfred University and at the Thermex Company in St. Petersburg, Russia, are developing a glass melt property database for the glass manufacturers who model glass melting and forming processes. The compositions being studied comprise six types of glass: container glass, float glass, fiberglass (E and wool types), low expansion borosilicate glass, and TV panel glass. The melt properties include gas solubility, density, thermal expansion, surface tension, viscosity (Newtonian

Table 4. Some Current Techniques for Studying Glass Surfaces<sup>a</sup>

Technique	Comments/general information	Characteristics measured
nuclear reaction analysis	detection of $\gamma$ -radiation from the nuclear reaction of $^{15}\text{N}$ and H	quantitative technique; analyzes light elements, including hydrogen, and concentration depth profile in hydration processes
X-Ray Scattering		density of the surface or films; surface and buried interface roughness; film thickness; distinction between physical roughness and chemical gradients at interfaces; chemical composition; and element-specific coordination number, bond distances, and oxidation states
secondary ion mass spectroscopy	SIMS can perform depth profiles with in-depth resolution of 0.2–5 nm range	analyzes modifications of the surface composition (aging, dealcalization, diffusion) and layers deposited on the surface (organic and inorganic) with lateral resolution of $\sim 0.1$ – $1\ \mu\text{m}$
fourier transform infrared spectroscopy	other FTIR spectral methods: DRIFT (diffuse reflectance infrared fourier transform), ATR (attenuated total reflection), and PA (photo-acoustic spectroscopy)	monitors the interaction of organic and inorganic coatings with inorganic glass substrates
atomic force microscopy	AFM probes the surface with a tip, $\sim 2\ \mu\text{m}$ long and $\sim 100\text{\AA}$ diameter, located at the free end of a cantilever 100–200 $\mu\text{m}$ long. Forces between tip and the surface cause the cantilever to deflect which is measured as the tip is scanned over the sample and a computer generates the surface topography	microscope and high precision 2D profilometer, lateral resolution $> 0.1\ \text{nm}$ and height resolution $> 0.01\ \text{nm}$ (glass structure, roughness and surface defects, corrosion and aging, fracture mechanics, and coatings on glass)
electron probe microanalysis	EPMA uses incident electrons to excite the glass surface with characteristic X-rays emitted	chemical information at or near glass surface; WDS (wavelength dispersive spectrometry) detects light elements
X-ray photoelectron spectroscopy		outermost composition $\sim 5$ – $10\ \text{nm}$

<sup>a</sup>Refs. 91,92.

and non-Newtonian), heat capacity, and radiative thermal conductivity (98). Full review of the model and database by selected CGR glass companies is expected by December 2003.

**3.1. Optical Properties.** Probably the most striking characteristic of conventional glasses is their transparency to visible light resulting from the

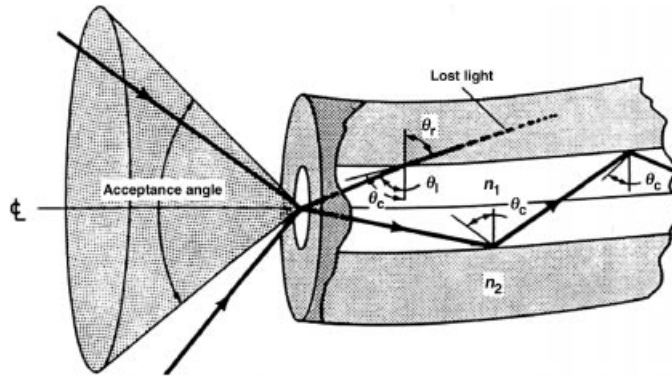


Fig. 12. Light guiding in a clad fiber (99).

absence of grain boundaries and light-scattering defects. The optical transparency of high purity silica glass made it possible to develop efficient optical fibers and devices. For practical light-transmitting fibers, a cladding glass with a lower refractive index,  $n$ , surrounds the core glass and light is guided through the core by internal reflection on the interface between the core and cladding. The difference in  $n$  between core and cladding determines the acceptance angle (or numerical aperture) for incoming light (see Fig. 12).

Optical glasses are usually described in terms of their refractive index at the sodium D line (589.3 nm),  $n_D$ , and their Abbé number,  $v$ , which is a measure of the dispersion or the variation of index with wavelength. Glasses with  $n_D < 1.60$  and  $v < 55$  are defined as crown glasses and those with  $n_D > 1.60$  and  $v < 50$  are defined as flint glasses (Fig. 13). A low dispersion is desirable in optical glasses used for lenses because dispersion causes chromatic aberration. Fluorophosphates, having absorption edges located well into the ultraviolet (uv), are examples of glasses with high Abbé numbers and low refractive indexes.

The loosely bound valence electrons make the greatest contribution to  $n$ , so large ions, such as Pb(II) or Bi(III), are added to glass to increase the refractive index. Glasses from the  $\text{PbO}-\text{Bi}_2\text{O}_3-\text{Ga}_2\text{O}_3$  have refractive indexes for visible wavelengths as high as 2.7. Other high index commercial glasses have 30–70%  $\text{TiO}_2$ , 10–50%  $\text{BaO}$  and 0–10%  $\text{ZrO}_2$  (wt%) plus small amounts of other oxides. Such compositions require high melting temperatures, 1500°C and above, which together with their high chemical corrosiveness toward refractories is a severe limitation to preparing these glasses by conventional melting methods. The distinguishing features of borate glasses, relatively high refractive index and low dispersion, are related to the large number of molecules in a unit volume,  $N$ , compared with those of the other glasses (100).

The addition of alkali or alkaline-earth oxides to a glass-forming oxide shifts the uv absorption edge to lower energies (longer wavelengths). Conversely, the range of uv transmission is enhanced when the cations in the glass have a high charge/radius ratio, indicating a stronger cation–oxygen bond. High purity fused  $\text{SiO}_2$  glass has been developed that is highly resistant to optical damage by

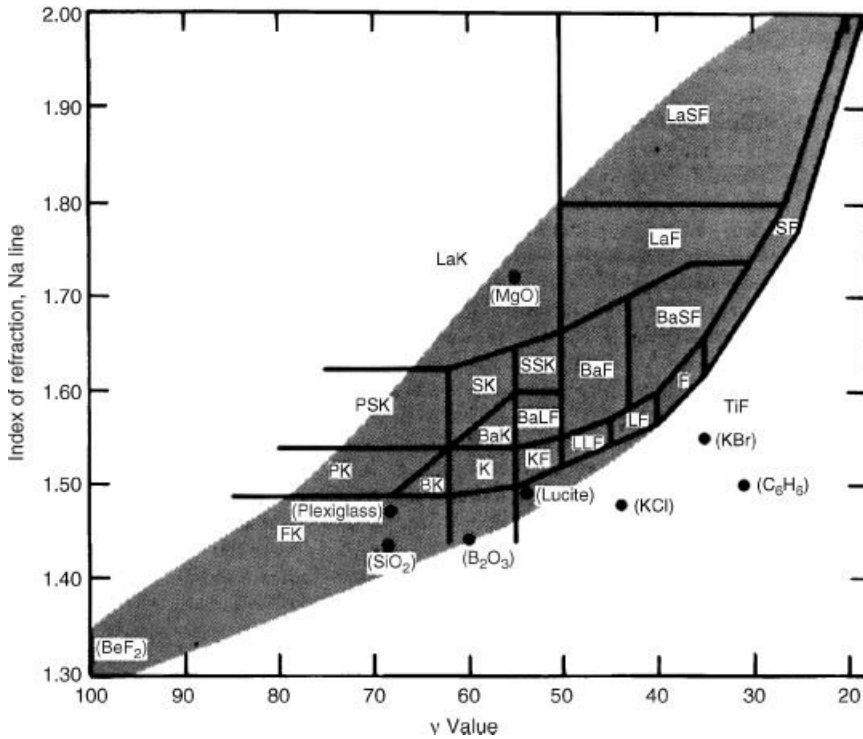


**Fig. 13.** Index of refraction vs dispersion and optical classification of glasses. The shaded area indicates region of glass formation. BaF=barium flint; BaK=barium crown; BaLF=light barium flint; BaSF=heavy barium flint; BK=borosilicate crown; F=flint; FK=fluorocrown; K=crown; KF=crown flint; LaF=lanthanum flint; LaSF=heavy lanthanum flint; LaK=lanthanum crown; LF=light flint; LLF=very light flint; PK=phosphate crown; PSK=heavy phosphate crown; SF=heavy flint; SK=heavy crown; SSK=very heavy crown; TiF=titanium flint.

uv (190–300-nm) radiation. The glass exhibits no optical damage after  $\sim 10^7$  pulses ( $350 \text{ mJ/cm}^2$ ) from KrF lasers at 248 nm and from ArF lasers at  $\sim 193 \text{ nm}$  (101). The addition of nitride ions to oxide glasses shifts the uv edge to longer wavelengths, probably because of the greater polarizability of the trivalent nitrogen. Nitride glasses, in contrast to conventional optical glasses, or fluoride optical glasses, possess a remarkable combination of desirable properties, including, high hardness, high refractive index, and high softening temperature (102).

In the visible region, absorption by additives such as transition metal or lanthanide ions is usually more important than contributions from the glass formers themselves. Several references discuss in detail the generation of color in glass (eg, Refs. 103–105). The coloration of glass by uv radiation from sunlight (solarization) results from the oxidation of transition metal ions in the glass. Optically pumped laser action has been observed for most lanthanide ions in a variety of glass systems. Large, high power neodymium glass lasers have been used for inertial confinement fusion experiments. The best glass laser systems have the following qualities: the absorption spectrum of the lasing ion

matches the spectrum of the pump radiation; the absorbed radiation efficiently produces excited-state ions; the excited state has a long lifetime; the probability of radiative decay is high; and the line width of the emitted radiation (fluorescence) is narrow. The line width of the fluorescence band of the lanthanide ion is affected by the glass matrix. In general, the smaller the field strength of the anions, the less the perturbation of the coordination shells of the fluorescing ion and the narrower the line width, ie, fluoride and chloride glasses promote narrower line widths than those seen in oxide glasses (106).

The visible transmission of photochromic glasses decreases with increasing frequency of light, and the effect is reversible. These glasses contain  $\sim 10$ -nm droplets of silver chloride, AgCl, or other silver halides doped with copper(I) ions. In the presence of uv radiation, the reaction  $\text{Ag(I)} + \text{Cu(I)} \rightarrow \text{Ag} + \text{Cu(II)}$  occurs, leading to the formation of small particles of silver causing the glass to darken (107).

Chalcogenide glasses such as  $\text{As}_2\text{S}_3$  are colored or even opaque, because of the small difference in energy between the conduction and valence bands. On the other hand, color in reduced amber glasses is the result of a  $\text{Fe}^{3+}-\text{S}^{2-}$  chromophore, not involving  $\text{Fe}^{2+}$  (108).

**3.2. Chemical Durability.** The chemical durability of glass is critical for many applications, including the performance of glass containers for food and beverages, pharmaceuticals, and corrosive chemicals; the retention of high transparency for optical components, including windows, exposed to ambient conditions; the use of glass as a long-term host for radioactive and hazardous materials; and the performance of bioactive glasses implanted in the body. Numerous reviews exist that describe the chemical interactions between glass and various environments (eg, Refs. 109–111).

**Silicate Glasses.** The leaching of alkali-containing silicate and borosilicate glasses in aqueous solutions is considered as two processes occurring in parallel: exchange of alkali ions for  $\text{H}_3\text{O}^+$  from the solution (controlled by diffusion of ions through a hydrated layer) and dissolution of the hydrated layer (controlled by surface reaction kinetics). The chemical durability of glass against reactions with aqueous solutions is determined by sample states and by corrosion conditions. Sample states include glass composition, mole fraction of crystalline phases, internal or applied stresses, surface roughness, phase separation, and homogeneity of powder or bulk for of the material. Corrosion conditions include relative humidity, gas surface reactants, pH of solution, initial and final composition of corroding solution, pressure and temperature of the system, and ratio of the corroded area to the volume of the corroding medium (112). As a first approximation, the durabilities of alkali silicate and alkali borate glasses in aqueous solutions can be estimated from thermodynamic calculations (113,114). This approach is useful for describing the major species in solution and has established qualitatively that (1) alkali silicate glasses are less durable than silica, (2) the solubility of alkali silicate glasses increases with increasing pH, and (3) the relative stability of alkali silicate and alkali borate glasses should increase in the order of modifier oxide as  $\text{K}_2\text{O} < \text{Na}_2\text{O} < \text{Li}_2\text{O}$ ; as observed experimentally. However, such calculations neglect kinetic processes such as formation of diffusive layers and reprecipitation of glass constituents, as well as structural features of the glass network.

Certain network modifiers and intermediate oxides (Table 2) reduce substantially the rate of attack on alkali silicate glasses (eg, alkaline earth ions,  $\text{Zn}^{2+}$ ,  $\text{Al}^{3+}$ ,  $\text{Zr}^{4+}$ ). Alkaline earth ions promote the formation stable leached layers, whereas  $\text{Al}^{3+}$ ,  $\text{Zr}^{4+}$  increase the thermodynamic stability of the glass. The outstanding chemical durability of borosilicate glasses, like Pyrex, in aqueous solutions is a result, in part, of phase-separated structures. The durability is dependent on the amount of network modifier, the amount of  $\text{B}_2\text{O}_3$ , and the thermal history of the glass.

The resistance of silica and silicate glasses to sodium vapor (as in the use of highway sodium lamps) has been studied by several authors (115). The attack of silicates by sodium vapor (as example of attack by alkaline vapors) is explained by diffusion of sodium into the glass and then reaction between sodium and the glass.

**Borate Glasses.** Boron oxide is highly soluble in water and borate glasses are very hygroscopic. The addition of alkali oxide increases the number of four-coordinated boron tetrahedra (up to  $\sim 30$  mol% alkali oxide), which strengthens the structure and increases the resistance to chemical attack. Further addition of alkali oxide produces nonbridging oxygens, decreasing the resistance to aqueous dissolution. Alkali silicate glasses usually dissolve in aqueous solutions following a diffusion process ( $t^{1/2}$  law,  $\text{pH} < 9$ , sufficiently short times) whereas alkali borate glasses display linear kinetics of dissolution (116). The basic difference is the ability of silicate glasses to form a diffusive layer for the transport of alkali ions which in turn controls the overall process.

Fritted glasses have become the common method of incorporating borates into glaze and vitreous enamels. Major benefits of borate use include reducing thermal expansion and improving durability of the glaze. Borate sources are mainly borax and colemanite, and common commercial forms (minerals; refined minerals; and synthetic compounds) such as boric acid and borax pentahydrate (117).

**Phosphate Glasses.** Many phosphate glasses have a chemical durability inferior to that of most silicate and borosilicate glasses. Metaphosphate glasses are most common and the metal ions that link neighboring phosphate anions are readily hydrated, causing the entire phosphate chain to be released into the aqueous environment (118). Iron phosphate glasses are an exception (119–121). Because of their unusually high chemical durability, iron phosphate glasses and zinc–iron phosphate glasses are of interest for nuclear waste immobilization. The most durable compositions have O/P ratios near  $\sim 3.5$  and so are considered pyrophosphate compositions. Additionally, iron phosphate glasses have low melting temperature, typically between 950 and 1150°C. Investigations of iron phosphate wastefoms obtained by adding different amounts of various simulated nuclear wastes to a base iron phosphate glass,  $40\text{Fe}_2\text{O}_3 \cdot 60\text{P}_2\text{O}_5$ , showed that these glassy wastefoms have a corrosion rate 100 times lower than a typical sodalime silicate glass. Generally, iron phosphate glasses can contain up to 40 wt% of certain simulated waste (122).

**3.3. Electrical Properties. Ion Conducting Glasses.** In alkali containing glasses, charge is carried by alkali ions moving from modifier site to modifier site, and so properties like conductivity are sensitive to composition (ie, the number of charge carrying ions) and structure (the nature of the modifier

site). Glasses with very high conductivities have been developed as electrolytes for solid-state batteries (123, 124). Superionic conducting glass systems include (for  $\text{Ag}^+$ )  $\text{AgI-Ag}_2\text{O-MoO}_3$ ,  $\text{AgI-Ag}_2\text{O-P}_2\text{O}_5$ ,  $\text{AgI-Ag}_2\text{O-B}_2\text{O}_3$ ; (for  $\text{Li}^+$ )  $\text{Li}_4\text{SiO}_4\text{-Li}_3\text{BO}_3$ ,  $\text{LiCl-Li}_2\text{O-B}_2\text{O}_3$ ; (for  $\text{Cu}^+$ )  $\text{CuI-Cu}_2\text{O-P}_2\text{O}_5$ ,  $\text{CuI-Cu}_2\text{O-MoO}_3$ ; and (for  $\text{Na}^+$ )  $\text{Na}_2\text{O-ZrO}_2\text{-P}_2\text{O}_5\text{-SiO}_2$  (125). For example, the  $\text{Na}^+$  ionic conductivities of the glass-ceramic  $\text{Na}_{4.1}\text{Sm}_{0.5}\text{P}_{0.4}\text{Si}_{2.6}\text{O}_9$  and  $\text{Na}_{4.1}\text{Y}_{0.25}\text{P}_{0.4}\text{Si}_{2.6}\text{O}_9$  are reported as  $4.78 \times 10^{-2}$  and  $2.79 \times 10^{-2}$  S/cm at  $300^\circ\text{C}$ , respectively (126,127). Glasses and glass-ceramics that do not contain alkali oxides have low bulk electrical conductivities under normal conditions that increase somewhat with temperature; such materials are used as high temperature insulators in electrical and radio engineering (128).

Electrical conductivity of glasses in the system  $\text{Li}_2\text{Cl}_2\text{-Li}_2\text{O-B}_2\text{O}_3$  has been measured by the complex impedance method at 100–20,000 Hz using three-electrode connection of the specimen in the circuit. There is a distinct increase in conductivity and decrease of the activation energy with increasing content of  $\text{Li}_2\text{Cl}_2$ . Increased content of  $\text{Li}_2\text{O}$  brings about a mild increase in conductivity and a mild decrease of activation energy (129). Electrical conductivity, Raman spectra, and the glass-forming region have been determined in borate glasses containing lithium sulfate. The relation between conductivity and composition is discussed with reference to the glass structure (130).

Anomalies in the  $(x)\text{AgI}\cdot(1-x)\text{AgPO}_3$  glasses ( $x \sim 0.3$ ) are observed in the electric properties, molar volume, and also local probes like the  $^{31}\text{P}$  nmr relaxation time. These anomalies can be explained in terms of the opening of percolative channels among the metaphosphate chains, which are subsequently filled by the dissociated  $\text{Ag}^+$  and  $\text{I}^-$  ions. An attempt to reconcile the different data on activation energy for dc-conductivity and  $T_g$  reported in the literature has been made (131).

Protonic conduction in  $10\text{P}_2\text{O}_5 \cdot 90\text{SiO}_2$  and  $20\text{P}_2\text{O}_5 \cdot 80\text{SiO}_2$  (mol%) glasses prepared by sol-gel processing have been investigated as a function of the content of molecular water adsorbed in the pores. The results show that the electrical conductivity varies exponentially with the reciprocal absolute temperature and increases with the increase of the content of the adsorbed molecular water. The double-bonded oxygen and the high affinity of phosphorus for oxygen make protons easy to release and transfer, which is favorable to the protonic conductivity (132). The  $\text{Cu}^+$  conducting glass-ceramics, in particular  $\text{CuTi}_2(\text{PO}_4)_3$  based materials having the Nasicon structure, have been described and use as  $\text{Cu}^+$  ion conductors for low temperature  $\text{O}_2$  sensors (133). The partial substitution of  $\text{Zn}^{2+}$  for  $\text{Ag}^+$  in  $\text{Ag}_4\text{P}_2\text{O}_7$  leads to the formation of a wide glassy domain of composition  $(\text{Ag}_4\text{P}_2\text{O}_7) \cdot (1-y)(\text{Zn}_2\text{P}_2\text{O}_7)$  ( $y = 0.20\text{--}0.87$ ) (134).

**Mixed-Alkali Effect.** In single alkali glass systems, different processes contribute to the electrical conduction at different temperature. In general, the ionic conduction is due to the motion of alkali ions and as a consequence, the electrical conductivity is expected to be proportional to the concentration of the alkali ions.

The substitution of a second alkali ion, at constant alkali content, in many phosphate, borate, and silicate glasses causes a decrease in the electrical conductivity up to five orders of magnitude. This is called the mixed-alkali effect (MAE), observed in ionic conductive glasses (135,136).

Table 5. **Electrical Conductivity at Room Temperature ( $\sigma_{300}$ ) for Some Phosphate Glasses<sup>a</sup>**

Glass composition	$\sigma_{300}$ ( $\Omega^{-1} \text{ cm}^{-1}$ )
80Fe <sub>2</sub> O <sub>3</sub> -20P <sub>2</sub> O <sub>5</sub>	$3 \times 10^{-10}$
V <sub>2</sub> O <sub>5</sub> -P <sub>2</sub> O <sub>5</sub>	$\sim 10^{-5}$
50Fe <sub>2</sub> O <sub>3</sub> -50P <sub>2</sub> O <sub>5</sub>	$\sim 10^{-10}$
20Fe <sub>2</sub> O <sub>3</sub> -30CaO-50P <sub>2</sub> O <sub>5</sub>	$\sim 10^{-12}$
50V <sub>2</sub> O <sub>5</sub> -60P <sub>2</sub> O <sub>5</sub>	$4.6 \times 10^{-10}$
40Fe <sub>2</sub> O <sub>3</sub> -60P <sub>2</sub> O <sub>5</sub>	$8 \times 10^{-12}$
Fe <sub>2</sub> O <sub>3</sub> -TeO <sub>2</sub> -P <sub>2</sub> O <sub>5</sub>	$\sim 10^{-8}$ - $10^{-14}$
Li <sub>2</sub> O-B <sub>2</sub> O <sub>3</sub> -P <sub>2</sub> O <sub>5</sub>	$\sim 10^{-7}$ - $10^{-6}$
(40-x)Fe <sub>2</sub> O <sub>3</sub> . xNa <sub>2</sub> O.60P <sub>2</sub> O <sub>5</sub>	$\sim 10^{-13}$ - $10^{-10}$
24Cs <sub>2</sub> O-26.8Fe <sub>2</sub> O <sub>3</sub> -49.5P <sub>2</sub> O <sub>5</sub>	$8.5 \times 10^{-11}$
20Fe <sub>2</sub> O <sub>3</sub> -20K <sub>2</sub> O-60P <sub>2</sub> O <sub>5</sub>	$3.0 \times 10^{-11}$
30Fe <sub>2</sub> O <sub>3</sub> -9Na <sub>2</sub> O-61P <sub>2</sub> O <sub>5</sub>	$8.9 \times 10^{-12}$

<sup>a</sup>Ref. 138.

As described by Day (135), the lower conductivity of mixed-alkali glasses has been attributed to changes in both the size of the alkali ions and to an interaction between different alkali ions and the glass network. The diffusion with memory model proposed by Bunde and co-workers (137) reproduces the variations of  $\sigma_{dc}$  as well as  $\sigma_{ac}$  conductivity in mixed-alkali (Na, K) silicate glasses. The studies of the alkali mixed effect have been related to the ionic conductivity in alkali silicate, phosphate, and borate glasses (Table 5) and there are little works on electronic conductive glass such as the studies in iron-phosphate glasses.

**Semiconducting Glasses.** Amorphous selenium and other chalcogenide glasses form the basis for the multibillion dollar electrostatic copying industry. Chalcogenide glasses can be switched between low and high conductivity states using an applied voltage. There are two types of switching: threshold and memory. In the case of threshold switches, a small current is required to maintain the ON (high conductivity) state. In contrast, memory switches remain on indefinitely in the absence of a current and require a short, high current pulse to return to the state. A typical glass for a memory switch contains Ge, Te, and either As, S, or Sb. The ON state in threshold switching is thought to arise from the saturation of charged defect centers.

Semiconductivity in oxide glasses involves polarons (conducting electrons in an ionic solid together with the induced *polarization* of the surrounding lattice). In oxide glasses the polarons are localized, because of substantial electrostatic interactions between the electrons and the lattice. Conduction is assisted by electron-phonon coupling, ie, the lattice vibrations help transfer the charge carriers from one site to another. Cations capable of multiple valences facilitate small-polaron conductivity. Vanadium and tungsten ions readily assume multiple valences, and vanadium oxide and tungsten oxide glasses exhibit some of the highest electrical conductivities of any oxide glass. Phosphate and tellurate(IV) glasses containing substantial amounts of multiple-valent transition-metal ions such as iron or copper are also semiconducting.

**3.4. Thermal Properties.** When a typical liquid is cooled, its volume decreases slowly until it reaches the melting point,  $T_m$ , where the volume decreases abruptly as the liquid is transformed into a crystalline solid. This phenomenon is illustrated by line A in Figure 1. If a glass-forming liquid is cooled below  $T_m$  (line B in Fig. 1) without the occurrence of crystallization, it is considered to be a supercooled liquid until the  $T_g$  is reached. At temperatures below  $T_g$ , the material is a solid. Faster cooling yields a less dense glass, as shown by line C.

Unlike the abrupt melting of a crystalline solid, the  $T_g$  is characterized by a continuous change in properties over a small temperature interval. When a solid glass is heated from below  $T_g$ , the volume and specific heat increase. As the  $T_g$  is reached, the rates of change of these quantities become greater, indicating that bonds are being broken and that some parts of the glass have become more mobile; ie, above  $T_g$  the behavior of the glass becomes more like that of the liquid phase.

The  $T_g$  of silicate glasses usually decreases as modifying oxides such as  $\text{Na}_2\text{O}$  are added because of the formation of nonbridging oxygen atoms. Although  $T_g$  is important regarding glass formation, other temperatures are more useful from a technological point of view. For example, the American Society for Testing and Materials (ASTM) (139) defines several characteristic temperatures in terms of viscosity (Fig. 14; working point (viscosity of  $10^3 \text{ Pa}\cdot\text{s}$ ), softening point ( $10^{6.6} \text{ Pa}\cdot\text{s}$ ), annealing point ( $10^{12} \text{ Pa}\cdot\text{s}$ ), and strain point ( $10^{13.5} \text{ Pa}\cdot\text{s}$ ) (140–142). The annealing point temperature is close to  $T_g$ , at which temperature the glass structure (and stresses) will relax in minutes. If annealing is carried out at the strain point, the reduction of stresses to acceptable levels takes  $\sim 4 \text{ h}$ .

The temperature dependence of the viscosity of a glass melt is non-Arrhenian and is often described by the Vogel-Fulcher-Tamman (VFT) equation

$$\eta = \eta_0 \exp\left(\frac{B}{T - T_0}\right) \quad (5)$$

where  $\eta_0$ ,  $B$ , and  $T_0$  are fitting parameters.

High silica glasses such as Pyrex have low CTE (coefficient of thermal expansion) and are used in applications requiring good resistance to thermal shock. Ultralow expansion  $\text{SiO}_2\text{--TiO}_2$  glasses have CTEs of practically zero, as do certain lithium-aluminosilicate glass ceramics, like Zerodur. Some applications, such as glass-to-metal seals, require glasses to have higher CTEs to match metals and other materials. Highly modified silicate glasses and glass-ceramics and phosphate glasses have been developed for high CTE ( $>10 \times 10^{-6}/^\circ\text{C}$ ) sealing applications.

The thermal conductivity of glass is dependent on lack of long-range structural order. The mean free path of a phonon in a glass is on the order of a few interatomic spacings, so phonons are damped out over very short distances, making glasses good thermal insulators, at least up to temperatures where radiative processes become dominant. Thermal conductivity increases when glasses are crystallized to form a glass-ceramic. On the other hand, the thermal conductivity of an aerogel is exceptionally low. Recent developments have combined this property of silica aerogels with polymer cross-linking to develop very high strength and very light materials, for potential applications in aerospace (143).

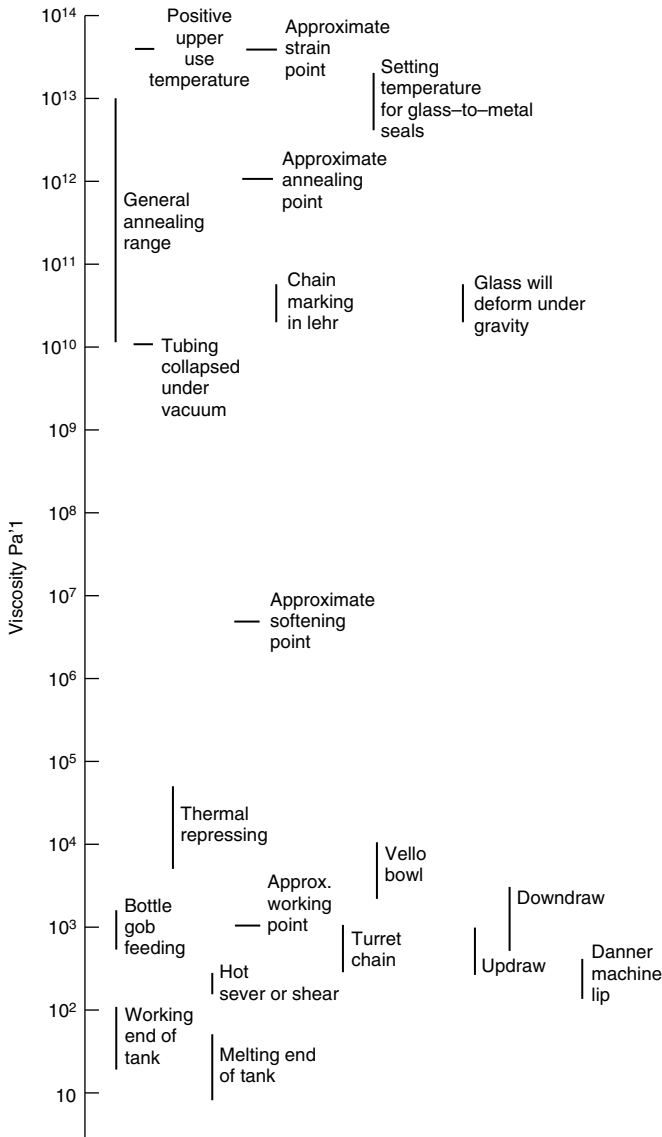


Fig. 14. Viscosity range of glass with relation to main processes.

**3.5. Mechanical Properties.** High strength glass fibers combine high temperature durability, stability, transparency, and resilience at low cost weight–performance. Various glass compositions have been developed to provide combinations of fiber properties for specific end-use applications. Tables 6 and 7 provide information on selected compositions. The mechanical properties of silica optical fibers have been studied extensively in recent years because of their use in optical technologies such as lightguides and in high energy laser applications (144,145).

Table 6. Composition Range of Commercial Glass Fibers, wt%<sup>a</sup>

Glass	A	C	D	E	M	S	EC/ Zglass		
							816	CEMFIL	ARG
SiO <sub>2</sub>	72–72.5	60–65	74.5	52–56	53.7	64.3–65	58	71	60.7
Al <sub>2</sub> O <sub>3</sub>	0.6–1.5	2–6	0.3	12–16		24.8–25	11	1	
B <sub>2</sub> O <sub>3</sub>		2–7	22.0	8–13					
CaO	9–10.0	13–16	0.5	16–25	12.9	0.01	22		
MgO	2.5–3.5	3–4		0–6	9.0	10.0–10.3	2.6		
Li <sub>2</sub> O					3.0			1	1.3
Na <sub>2</sub> O	13–14.2	7.5–12	1.0	0–1		0–0.27	1.0	11	14.5
K <sub>2</sub> O		0–2	0–1.3						2.0
TiO <sub>2</sub>				0–0.4	7.9–8.0			2.2	
CeO <sub>2</sub>					3.0				
ZrO <sub>2</sub>					2.0			16	21.5
BeO					8.0				
ZnO							2.8		
Fe <sub>2</sub> O <sub>3</sub>				0.05–0.4	0.5	0.02			
F <sub>2</sub>				0–0.5					
SO <sub>3</sub>	0.7		0.1						

<sup>a</sup>Ref. 146.

**Strength and Fatigue.** The “inert intrinsic strength” of silica fibers is ~14 GPa (147). This term has been operationally defined as the strength of flaw-free glass measured under conditions where no delayed failure is allowed. This strength has been measured for few other glass compositions. For example, iron-phosphate glasses for use as nuclear waste glass (148) show high Young’s modulus and tensile strength. The combination of high strength and good chemical durability of the iron-phosphate glasses are valuable advantages for potential technological applications (149).

While the measurement of MOE (modulus of elasticity) of silicate glasses is straightforward, the calculation of strength is not similarly possible as strength is a “weakest link” property. It depends not on the average properties of the sample (ie, properties of the network), but on the weakest portion of the sample. In the case where flaws are present, the strength is governed by the critical stress as in the Griffith equation:

$$\sigma = (E\gamma/c)^{1/2} \quad (6)$$

or as in the fracture mechanics modification:

$$\sigma = K_{IC}/Yc^{1/2} \quad (7)$$

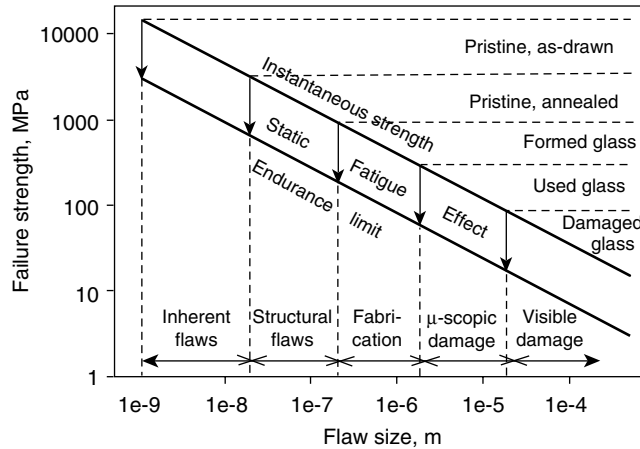
applicable to the behavior of specimens containing sharp flaws or cracks of length  $c$ . The parameter  $Y$  describes the geometry of the tip,  $E$  is the MOE (modulus of elasticity/Young’s modulus),  $\gamma$  is the fracture surface energy, and  $K_{IC}$  is the fracture toughness. Cracks concentrate the stress so that it may be orders of magnitude greater at the crack tip than the applied stress. If the applied stress is not the critical stress, then failure will not occur instantaneously. If there is

Table 7. Properties of Commercial Fibers<sup>a</sup>

Property	Fiber Type					
	A	C	D	E	M	S
specific gravity	2.50	2.49	2.16	2.54–2.55	2.89	2.48–2.49
refraction index at 589.3 nm	1.512	1.541	1.47	1.547	1.635	1.523
dielectric constant at 21°C, 10 <sup>6</sup> Hz	6.90	6.24–6.30	3.56–3.62	5.87–6.6		4.53–4.60
thermal conductivity, 10 <sup>-3</sup> cal-cm/°C-s					2.3	
specific heat, cal/g°C		0.19–0.21	0.175	0.192		0.176
linear expansion coefficient, 10 <sup>-7</sup> °C <sup>-1</sup>	90	70–72	31	49–60	57	29–50
liquidus temperature, °C				1065–1120		1500
fiberizing temperature, °C	1280			1270–1300		1565
strain point, °C		1025	890	1140		1400
annealing point, °C		1090	970	657		810
softening point, °C	1285–1330	1380–1385	1420	1555		1775–1778
hardness, Vickers, 10 <sup>6</sup> psi				0.76		0.82
Young's modulus, GPa	72.5	70	51.7	72.4–76	110	84–88
Poisson's ratio				0.10–0.22		
virgin tensile strength at room temperature, MPa	2414	2758–3103	2414	3500	3500	4600
virgin tensile strength at liquid N <sub>2</sub> temperature				5900		8300
fracture tough- ness, MPa · m <sup>1/2</sup>				0.90		1.2
stress corrosion susceptibility exponent				28–31		40
weight loss % of 14 mm diameter fiber after 1 h boil in H <sub>2</sub> O	11.1	0.13		1.7		
1N H <sub>2</sub> SO <sub>4</sub>	6.2	0.10		48.2		
0.1N NaOH	12–15.0	2.28		9.7		

<sup>a</sup>Ref. 146.

moisture present in the environment, subcritical slow crack growth (fatigue) will occur, which is of major consequence in silica lightguide fibers. The effects of crack size (including those generated from typical processing and handling) and fatigue processes on glass strength are summarized in Figure 15.



**Fig. 15.** Effects of crack size (including those generated from typical processing and handling) and fatigue processes on strength in silica glass (150).

**Flaw Generation and Strengthening.** Glass surfaces may be damaged by either mechanical means or by chemical means, ie, a chemical interaction that leads to mechanical degradation. In this case, a solid, liquid, or gas phase may react with the glass surface forming a new product or developing residual stresses due to bonding materials with different thermal expansion coefficients.

The most common techniques for improving the strength of glass surfaces are based on the fact that failure in glasses occurs in tension that in turn is the result of stress concentrations due to surface flaws. Thus the reduction of tensile stresses at the surface by superposition of a surface compression is usually very effective (151,152). In thermal tempering, the rapidly cooled surface sets up before the more slowly cooling interior. As the interior proceeds to cool, it places the already set surface into compression. Ion-exchange strengthening is a process commonly used where large ions ( $K^+$ ) are exchange for smaller ions ( $Na^+$ ) in the glass surface at temperatures below the annealing temperature. The increased volume required leads to a surface compression. Alkali-alumino silicate glasses provide high rates of ion exchange with relatively little stress relaxation (153). In general, the surface compressive stress for thermal tempering is  $\sim 100$  MPa, while for ion exchange is  $\sim 1000$  MPa. Ion exchange produces a very steep stress gradient while in thermally tempered glass the compressive layer may extend  $>20\%$  of the thickness.

The use of coatings is another way of preventing the formation of flaws or flaw growth. Polymer-based materials are usually applied to glass containers both for mechanical protection and for decoration. Lightguides are also coated with a polymer that must be applied in line as the fiber is drawn.

#### 4. Manufacture

Glasses can be prepared by methods other than cooling from a liquid state, including from the solid-crystalline state (ie, lunar glasses) and vapor phases

Table 8. Technical Innovations of the Twentieth Century<sup>a</sup>

basic glass processing	float glass process ribbon machine for glass bulbs owens suction machine (containers) Danner process for making glass tubing
fiberglass	continuous melting of optical glass continuous glass fibers steam blown glass wool rotary fiberizing
specialty glass items	glass ceramics radiant glass–ceramic cooktops glass microspheres laminated glass borosilicate laboratory and consumer glassware large, flat-glass TV tubes automotive solar control electrically heated windshield automotive tempered window 2.5 mm thick photochromic and photosensitive glass ceramic and glass foodware safety
glass lasers and fiber optics	glass lasers low loss optical fibers erbium-doped optical fiber amplifiers ultraviolet-induced refractive index changes in glass fiber optic sensors
other	bioactive glasses, ceramics and glass–ceramics nuclear waste glasses chemical tempering of glass products (ion exchange)

<sup>a</sup>Ref. 157.

and by ultrafast quenching procedures: (1) melt spinning, in which molten metal is ejected onto a rapidly spinning cylinder to form thin ribbons; (2) splat quenching, in which the melt is smashed onto an anvil by a compressed-air-driven hammer; (3) twin-roller quenching, in which the melt is forced between two cylinders rotating in opposite directions at the same speed; (4) laser glazing, in which a short, intense laser pulse is focused onto a very small volume of a sample; and (5) laser spin melting in which a rapidly rotating rod of the starting material is introduced into a high power laser beam, eg, a CO<sub>2</sub> laser, causing molten droplets to spin off and form into small glass spheres (154). Table 8 summarizes the technical innovations of the twentieth century concerning glass processing and new glass developments. The technological aspects of glass making have been compiled, eg, by Tooley (155) and by Scholes (156).

Glass manufacture requires four major processing stages: batch preparation, melting and refining, forming, and postforming (Fig. 16). Silica is the basis of most commercial glasses; however, it has a high melt viscosity, even at temperatures close to 2000°C, making melting and working extremely difficult. Container and flat glass compositions are based on the Na<sub>2</sub>O–CaO–SiO<sub>2</sub> system (Table 9) with addition of other minor components to improve glass formation, lower liquidus temperature, and improved durability. Borosilicate glasses have low expansion coefficient and good thermal shock resistance that makes them

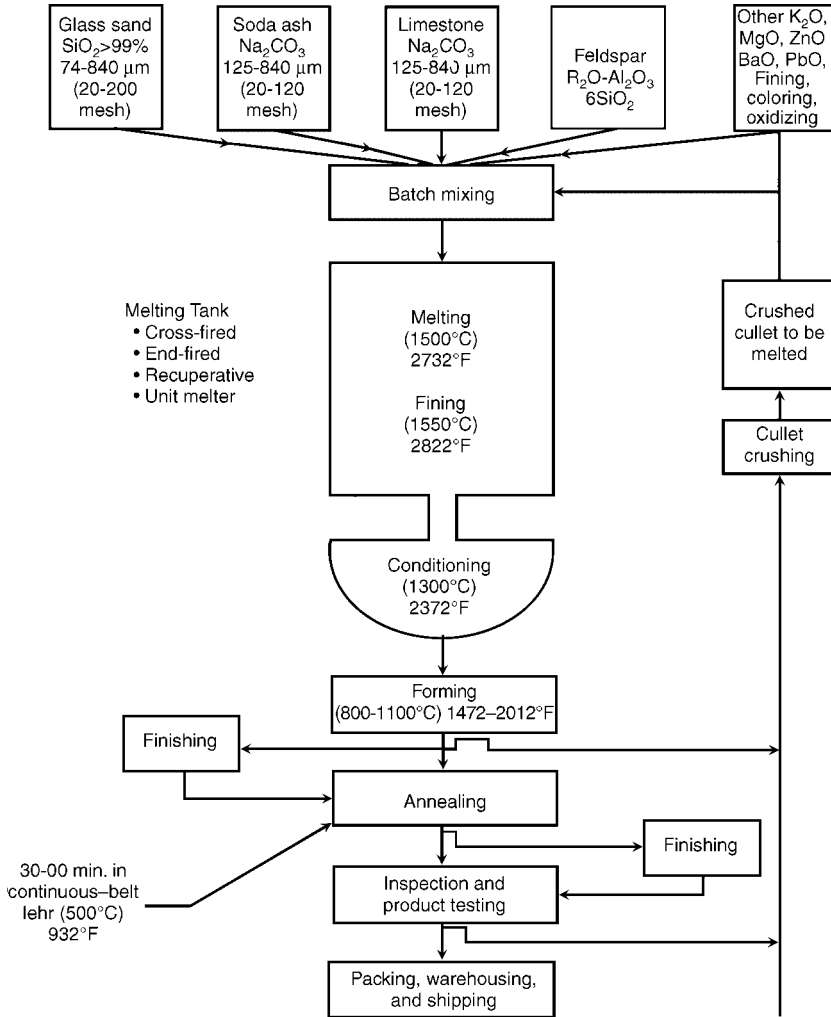


Fig. 16. Overview of glass manufacturing (158).

suitable for laboratory and kitchen ware. E-glass (Table 6) is an alkali free  $\text{SiO}_2-\text{Al}_2\text{O}_3-\text{CaO}-\text{B}_2\text{O}_3$  glass used for electrical insulation.

**4.1. Glass-Manufacturing Processes. Batch Preparation.** This step refers to mixing and blending of raw materials to achieve a desired glass composition. The glass batch contains glass formers, fluxes, fining agents, stabilizers,

Table 9. Typical Glass Compositions<sup>a</sup>

Glass	$\text{SiO}_2$	$\text{Na}_2\text{O}$	$\text{K}_2\text{O}$	$\text{CaO}$	$\text{MgO}$	$\text{PbO}$	$\text{Al}_2\text{O}_3$	$\text{B}_2\text{O}_3$	other
container glass	72.7	13.8	0.5	11.0	0.1		1.6		0.3
flat glass	72.8	12.7	0.8	8.1	3.8		1.4		0.4
borosilicate	80.1	4.5	0.3	0.1			2.6	12.2	0.2
lead crystal	54.0	0.2	12.2			31.8	0.1	0.5	0.4

<sup>a</sup>Ref. 158.

Table 10. Common Glass Components

glass formers	boron oxide ( $B_2O_3$ ) from borax or boric acid or from ores (colemanite, raserite, ulexite) feldspars (Ca, Mg, Na, or K alumina silicates), source of alumina lead oxides (PbO/litharge, $Pb_3O_4$ /red lead), PbO source for lead glasses silica sand ( $SiO_2$ ); 30–10 mesh size for containers, <200 mesh for fibers
fluxes	cryolite ( $Na_3AlF_6$ )—also opacifier in opal glasses lithium carbonate potash ( $K_2CO_3$ ), $K_2O$ source soda ash ( $Na_2CO_3$ ), $Na_2O$ source spodumene (Li-aluminosilicate), melting accelerator
stabilizers	alumina ( $Al_2O_3$ ) aplite (K, Na, Ca, Mg-alumina silicate), alumina source aragonite–limestone–calcite ( $CaCO_3$ ), CaO source barium carbonate, BaO source for specialty glasses dolomite, $CaMg(CO_3)_2$ , CaO, and MgO source litharge (PbO) magnesia (MgO) nepheline syenite (nepheline and feldspars), alumina source strontium carbonate zinc oxide zirconia ( $ZrO_2$ )
fining agents	antimony oxide ( $Sb_2O_3$ ); also decolorizing agent arsenic oxide ( $As_2O_3$ ); also decolorizing agent barite ( $BaSO_4$ ); also flux and source of barium calumite slag (Ca–Al–silicate by-product of the steel industry) gypsum ( $CaSO_4 \cdot 2H_2O$ ) salt cake ( $Na_2SO_4$ ); also melting aid sodium antimonite ( $2Na_2O \cdot 2Sb_2O_5 \cdot H_2O$ ); also decolorizing agent sodium nitrate ( $NaNO_3$ ); also oxidizing agent
colorants	cobalt oxide ( $Co_2O_3 \cdot CoO$ ), strong blue colorant chromite ( $FeO \cdot Cr_2O_3$ ), used for green bottles iron oxides–rouge ( $FeO$ , $Fe_2O_3$ , $Fe_3O_4$ ) manganese dioxide–pyrolusite ( $MnO_2$ ) nickel oxide potassium dichromate ( $K_2Cr_2O_7$ ), colorant in artware pyrite (iron sulfide), colorant in amber glass selenium, decolorizing agent, also used in colored glasses tin oxides ( $SnO$ , $SnO_2$ ), used in artware
others	caustic soda (NaOH solution), for batch wetting cerium oxide (CeO), uv absorber for specialty glasses fluorspar ( $CaF_2$ )

and sometimes colorants (Table 10). The main raw material is high quality silica sand (essentially quartz), which has to be carefully selected for several reasons. The cost of transporting sand is four to five times the cost of the material, and finer sands are more expensive than coarser sands. Using the incorrect size sand can create melting and product quality problems. Other major sources for glass formers are feldspar (a source of alumina) and borax or boric acid (manufacture of high temperature glass, Pyrex, fiberglass).

Fluxes are added to lower the temperature at which the batch melts. Soda ash ( $Na_2CO_3$ ) is the main source of sodium oxide in glassmaking. Stabilizers

improve the chemical stability of the glass. Common stabilizers include limestone (calcite, 95%  $\text{CaCO}_3$ ), alumina, magnesia and barium carbonate. Fining agents are used to minimize seeds, blisters, and bubbles. These agents include sulfates, arsenic, antimony, fluorides, phosphates, and chlorides. The use of  $\text{Na}_2\text{SO}_4$  and a reducing agent is the most common fining system used for soda–lime–silica glasses. Fining is a complex process that depends on the glass viscosity and composition, raw materials, and the redox conditions. There are a number of additives used to impart color or unique properties to the glass. Common colorants include compounds of Fe, Cr, Ce, Co, and Ni. Amber glass is produced using  $\text{Fe}_2\text{S}$  (iron-pyrite). Both  $\text{CoO}$  and  $\text{NiO}$  are used to decolorize the yellow-green tint from iron-contamination. When mixed with Fe and Co, Se creates a glass with a bronze color.

Another raw material is cullet or recycled glass, obtained from within the plant and/or from outside recycling firms. Cullet may constitute 10–80% of the batch. Cullet from outside recycling may be contaminated or of inconsistent quality and it is not generally used in applications where higher quality is required (ie, float glass). Ceramic contaminants do not dissolve in the glass and remain as inclusions in the final ware. Cullet is less costly than virgin materials and reduces the energy required for melting.

**Melting and Refining.** Commercial melting refers to forming a homogeneous molten glass from the raw materials at temperatures between 1430 and 1700°C (2600–3100°F). As the batch is heated a series of processes and chemical reactions occur, including melting, dissolution, volatilization, and oxidation–reduction (redox reactions). The batch undergoes a four-step process in the melting furnace: melting, refining, homogenizing, and heat conditioning (Fig. 17). Melting should be complete before the batch has gone through the first one-half of the furnace. Melting rate depends on the furnace temperature, composition of the batch, grain size of the batch ingredients, amount and grain size of cullet, and homogeneity of the batch.

During refining (or just fining), gas bubbles are eliminated from the molten glass. The refining section of the furnace is usually separated from the main

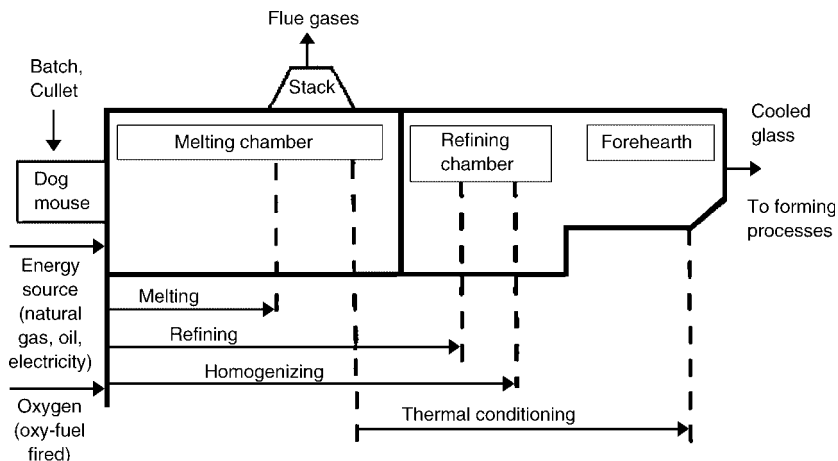


Fig. 17. Melting and refining processes (158).

melting section by a bridgewall, while glass flows through a wall opening called the throat. Gas bubbles ( $O_2$ ,  $SO_2$ ,  $H_2O$ ,  $N_2$ , and  $CO_2$ ) are dissolved in the glass depending on the type of glass and raw materials. Refining helps to remove these bubbles. Compounds such as  $Na_2SO_4$ ,  $NaCl$ , and  $CaF_2$  are used as refining agents. The use of arsenic and antimony is decreasing for environmental reasons. Glass inclusions are also eliminated or reduced during refining.

Homogenizing occurs throughout the melting chamber and is finished when the properties of the glass meet a given set of specifications. Factors affecting homogeneity include temperature, time, batch composition, degree of mixing, and possibility of reactions with the refractory furnace system. During thermal conditioning, the glass is stabilized and brought to a uniform temperature. Thermal conditioning begins after the glass reaches its highest average temperature in the furnace; after this time it will begin cooling to the working temperature and forming.

**Glass Forming.** In this stage the molten glass begins its transformation into the final shape. Molten glass can be molded, drawn, rolled, cast, blown, pressed, or spun into fibers. For example, nearly all flat glass is produced today by the float glass process. In this process, molten glass ( $\sim 1065^\circ C$ ) flows horizontally from the forehearth onto a pool of molten tin. As the hot glass passes over the molten tin it conforms to the tin surface perfectly flat and develops a uniform thickness with no distortion.

Glass containers are formed by transferring the molten glass into molds by a method called gob feeding. During gob feeding, the weight and shape of the molten glass gobs are controlled. The temperature of the molten glass is very important to the formation of gobs. If the glass is too cool, the glass is too viscous to transfer properly. Today most container manufactures use the IS (individual section) machine for automatic gob feeding. The IS machine is capable of handling a variety of types and sizes of molds, and can produce containers at rates  $>100/\text{min}$ . The Owens Illinois Company has developed an IS machine with four banks of 10 "individual sections" that can produce over 500 bottles/min.

Continuous glass fibers were first manufactured during 1935 in Newark, Ohio and started a revolution in reinforced composite materials that has grown to consumption  $>3 \times 10^6$  tons/year worldwide. Raw materials for glass fibers include silica, soda, clay, limestone, boric acid, and fluorspar, which are melted in a furnace and refined during lateral flow to the forehearth. The molten glass flows to Pt/Rh alloy bushings through individual bushing tips with orifices ranging from 0.76 to 2.03 mm and is rapidly quenched and attenuated in air to yield fine fibers ranging from 3 to 24  $\mu\text{m}$ . Mechanical winders pull the fibers at linear velocities up to 61 m/s over an applicator that coats the fibers with an appropriate chemical sizing to aid processing and performance of the end product. A summary of forming methods and energy considerations, with a comprehensive review, has been issued by the U.S. Department of Energy (DOE) (158).

**Postforming and Finishing Operations.** After taking its final shape, the glass product may be subjected to curing–drying (fiber glass products), tempering, annealing, laminating, and coating, polishing, decorating, cutting, or drilling. Annealing is the process of slow cooling to release stresses by the time the glass product reaches room temperature. Strain and stresses are dependent on how fast the glass is cooled through  $T_g$ .

Annealing is done for all types of glasses except fibers. Tempering is used to impart strength to glass sheets. It is accomplished by heating annealed glass just below its softening temperature, and then rapidly quenching the glass with air. The rapid cooling allows the glass surface to be in compression in relation with the internal regions that continue to flow. The result is increased resistance to bending failure.

After annealing, some types of flat glass are subjected to tempering, particularly automotive and some architectural glass. Glass that is going to be used for automotive (ie, doors, windshields) may require bending before tempering. The glass is then heated and bent to required shape, and quenched. Laminating, typical for windshields, is the process of placing an organic plastic film between two or more layers of glass. If the glass is broken, the pieces are held in place by the plastic. All glass containers are annealed after forming much similar in a way to that used for flat glass. However, nonuniform temperature distributions may occur due to variation in glass thickness and shape complexity.

**4.2. Glass Melting Tanks. Furnaces.** In general, furnaces are classified as discontinuous or continuous. Discontinuous furnaces are used in small glass-melting operations (small blown and pressed tableware and specialty glasses) and are operated for short periods of time. In continuous furnaces, the glass level remains constant, with new batch materials being constantly added as molten glass is removed. Continuous furnaces are classified into four categories (Table 11): direct-fired, recuperative, regenerative (Fig. 18), and electric melting: continuous furnaces can be fired by natural gas, electricity, or a combination of both. In natural gas furnaces, the gas is burned in the combustion space above the molten glass and the transfer of energy occurs through radiation and convection. Electricity is introduced using electrodes that are placed directly into the molten glass.

Several techniques are being used to increase the furnace production capacity optimizing capital-intensive changes. These include electrical boosting, oxy-fuel firing, and preheat of the batch and cullet. These methods may also lower operating costs and improve the environmental performance of the furnace. Electric boost typically provides  $\sim 10\text{--}15\%$  of the energy requirements in a furnace and it is mostly used to increase productivity in an existing furnace, without increasing air emissions or making major changes to the furnace. Preheat of the cullet and batch is done using a separate burner or with heat available from the furnace exhaust. Since the gas is hot when it enters the furnace, less energy is required to reach melting temperatures. However, increased emissions can result from increase cullet and batch preheating. New methods are being tried, such as Praxair's technology (160) where batch-cullet is fed at the top of the preheater and "rains" through a heat exchanger. The batch-cullet particles are deflected by internal baffles and are in direct contact with rising hot flue gases.

Oxyfuel firing is used to increase combustion efficiency and reduce energy requirements. In melting furnaces, natural gas reacts with air ( $\sim 21\% \text{O}_2$  and  $78\% \text{N}_2$ ) where the nitrogen absorbs large amounts of heat, leaving the furnace stack at high temperatures as  $\text{NO}_x$ . The use of oxygen (either air-enriched or pure  $\text{O}_2$ ) reduces stack gas volumes and heat losses. However, it has been found that there is an increase in  $\text{NaOH}$  vapor concentration ( $\sim$ three times

Table 11. Furnace Types for Glass Melting

<i>Discontinuous furnaces<sup>a</sup></i>	
pot furnace	glass is melted in a refractory pot inside a furnace. open pots are exposed to flame and gases and have capacities of ~50–200 kg of glass. Closed pots may have larger capacity and are used for melting lead crystal glass and colored glasses.
day tanks	small units where the charging and melting cycle is repeated daily. They are used for specialty glasses including opal, ruby, crystal and sodalime glasses.
<i>Continuous furnaces<sup>b</sup></i>	
direct-fired furnaces (unit melters)	units fired with natural gas producing 20–150 ton/day. The burners are controlled to generate convection currents, which create a longitudinal temperature gradient along the furnace and glass melt. They are used in cases where glass components could degrade regenerator refractories (ie, specialty glasses, borosilicates).
recuperative furnaces	refer to direct-fired furnaces that have been fitted with recuperators to recover heat from exhaust gases; recovering heat doubles the thermal efficiency of the furnace; they are used in small operations (ie, insulation fiber).
regenerative furnaces	most common furnace in the glass industry, with capacities of 100–1000 ton/day. The furnace heat is collected in a regenerator which is used to preheat combustion air (as high as 1260°C) and achieve higher energy efficiency. <i>End-port regenerative furnaces</i> use side-by-side ports located in the back wall of the furnace with the flame entering through one port and traveling in u-shape over the glass melt from one side. Regenerators are located next to each other against the backwall of the furnace. <i>Side-port regenerative furnaces</i> have exhaust ports and burners placed on opposing sides of the furnace along with two regenerators, one on each side, with the flame traveling from one side to the other (Fig. 18).
all-electric melters	These furnaces take advantage of the conductivity of molten glass (the furnace must first be heated with fossil fuel and the temperature raised prior to electrical melting). Molybdenum electrodes are embedded in the bottom or sides of the furnace, and pass electrical current through the refractory chamber, melting the raw materials.

<sup>a</sup>Used for small operations, <5 ton/day.

<sup>b</sup>Used for larger operations over a period of years.

higher) compared to gas–air firing. This increase in soda vapor is detrimental to superstructure refractories.

The trend toward using oxyfuel firing is steadily increasing (161) as an oxyfuel furnace can produce the same amount of glass as with gas–air, but at lower fuel input. The glass industry is using today oxyfuel burners that require low maintenance, non-water cooled burners capable of firing up to 3000 kW (~10 × 10<sup>6</sup> Btu/h). When regenerative furnaces (Fig. 18) are converted to oxyfuel firing, the regenerator refractory structure is not needed, eliminating the exhaust volume by as much as 75% (158).

*Refractories for the Glass Industry.* Today, continuous furnaces are expected to last up to 10 years in operation. Glass-contact refractories have to

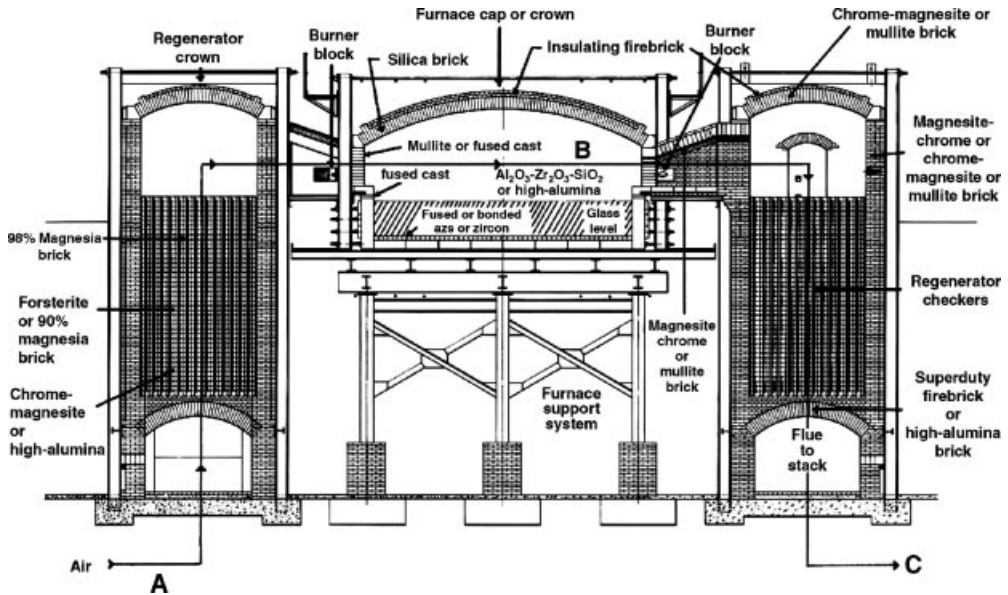


**Fig. 18.** Cross-section of typical regenerative sideport glass-melting tank. Gas and heated air enter at inlet A and the mix goes then to the burner blocks. The flame goes into the furnace across the top of the glass batch (B) while exhaust gases are withdrawn through the regenerator C. After a 15–20-min cycle, the process is reversed (from C to A) which allows efficient use of energy (159).

be carefully selected to improve furnace life minimizing side reactions that would lead to glass defects (162,163). At the flux line (glass level), surface tension and density driven flows at the combustion-atmosphere–refractory–molten-glass interface increases the refractory corrosion. Bubbles act similarly and promote “upward drilling” into downward facing surfaces such as throat, forehearth entry blocks, and any horizontal joints. Low porosity fusion-cast refractories (ie, AZS/alumina–zirconia–silica,  $\alpha/\beta$ - $\text{Al}_2\text{O}_3$ ) are used for glass contact applications; however, these refractories show high thermal conductivity. Insulation is essential except where corrosion is rapid as at the flux line where either external air or water cooling is used.

Floor refractories temperatures are lower than for sidewalls. However, molten metallic contaminants (from cullet materials) can drill into the refractories, penetrating even joints and attacking down to insulation layers. Superstructure refractories must resist batch dust, gas corrodants, fuel ash, and thermal shock and erosion by flames. Silica is commonly used, as it has low cost, high hot strength, and high corrosion resistance. However, for oxyfuel firing, fusion cast  $\beta$ - $\text{Al}_2\text{O}_3$  is used as it is highly resistant to soda vapor (164). Bricks in the regenerators are subjected to a similar attack as the superstructure, and with a cycling of temperature and corroding gases. Magnesium oxide refractories are normally used at the top of the regenerator although fused cast AZS refractories are also used. Aluminosilicate refractories are used where temperatures are lower. Figure 18 summarizes the location and use of main refractories in a melter

Table 12. Selected Refractories Used in the Glass Industry

Furnace section	Refractory	Composition, wt%						Apparent porosity, %	Density kg/m <sup>3</sup>	PCB <sup>a</sup> °C	MOR MPa	Applications
		ZrO <sub>2</sub>	Al <sub>2</sub> O <sub>3</sub>	SiO <sub>2</sub>	MgO	Cr <sub>2</sub> O <sub>3</sub>	Other					
super-structure	silica	<0.5		~96			2.5–3 CaO	~20	1850	1590–1650	3.4–7	crown <sup>b</sup>
	fused cast α,β-alumina	95		0.5–1			4 R <sub>2</sub> O <sup>c</sup>	2	3200–3400	1870	24.5	crown
	mullite sillimanite	60–80		18–37			1–6 R <sub>2</sub> O and Fe <sub>2</sub> O <sub>3</sub>	14–24	2200–2600		9–14	crown, backwalls, brestwalls
glass contact	standard fused cast AZS <sup>d</sup>	32–36	48–53	11–17			1–2 R <sub>2</sub> O	0–1	3400–3550	~1750		glass contact and regenerator <sup>e</sup>
	high ZrO <sub>2</sub> O, AZS	39–41	45–48	10–13			1 R <sub>2</sub> O	0–1	3600–3700	~1750		glass contact and super-structure <sup>e</sup>
	ZrO <sub>2</sub> AZS fused cast α,β-alumina dense chrome	92–96 0–3.5	0.5–2.5 95	3–5 0.5–1			0–0.5 R <sub>2</sub> O 4 R <sub>2</sub> O ~TiO <sub>2</sub>	0–1 2 <18	5100–5500 3200–3400 ~4000	~1750 1870 >1650	24.5 44	glass contact furnace throats fiberglass furnace throats <sup>f</sup>
regenerators	MgO	~2		0.3–0.6 <sup>g</sup>	~98		~1 CaO, ~0.2 Fe <sub>2</sub> O <sub>3</sub>	17–22	2800–2900	>1760	10–28	checkers <sup>h</sup>
	mag-chrome bricks	16–27	4–8		27–53	12–28	8–14 Fe <sub>2</sub> O <sub>3</sub>	14–25	1600–3330	1540–1650	2.8–17	regenerators and crown
other	fused silica			98–99			1 CaO	11–15	1900	1650	3.4–5.5	burner blocks, special shapes
	fused silica castables insulation firebrick (IFB)	34–36		~99 56–58			6–10 R <sub>2</sub> O and Fe <sub>2</sub> O <sub>3</sub>	15–18 63–77	1840–1970 600–900	1090–1430	0.7–1.2	crown repair <sup>i</sup> external insulation

<sup>a</sup>Pyrometric cone equivalent (165).

<sup>b</sup>Ref. 166.

<sup>c</sup>Alkalis.

<sup>d</sup>Alumina zirconia silica refractories.

<sup>e</sup>Ref. 167.

<sup>f</sup>Ref. 168.

<sup>g</sup>Amount of silica affects whether the refractory is direct bonded or chemical bonded (SiO<sub>2</sub>CaO ratio).

<sup>h</sup>Ref. 169.

<sup>i</sup>Ref. 170.

while Table 12 summarizes some useful properties of refractories for the glass industry.

A refractories database is being developed as part of a multiuniversity–National Science Foundation program (within the NSF, Technology, Engineering, and Mathematics Education Digital Library Program) creating a digital library of ceramic microstructures (DLCM) (171). This library will provide researchers and engineers with digital images to illustrate microstructures of a wide variety of functional ceramics. The DLCM will serve also as input to the object oriented finite element code, OOF, developed at the National Institute of Standards and Technology (NIST), which has been designed to calculate macroscopic properties from digital microstructure images (real or simulated) (172). The University of Missouri-Rolla will begin to supply information in the Refractories Materials category, starting with refractories for the glass industry (167).

**Sensors and Controls for Glassmakers.** On-line sensors provide a direct measure of some molten glass property: glass flow, melting rate, viscosity, strength, color, refractory corrosion, emissions, etc, which need to be controlled to optimize the glass-melting process. For best applications, a sensor should not change the environment or affect the property being measured; and the sensor should not be degraded by the environment. The advent of nontraditional methods of melting glasses will also require nontraditional on-line sensors under very demanding conditions. This has prompted the U.S. DOE to invest heavily in what is called “The Industries of the Future” to help ensure that R&D resources are strategically allocated to maximize benefits (173).

The higher demand on quality of glass products (ie, flat panel displays), the need to meet future legislation on wastes and emissions, and the need to improve energy efficiency require new sensors for process control. By developing sensors capable of withstanding the high temperature and severe corrosive environment, the glass-making process can become more energy efficient and cost effective. The status of sensor technology is presented in Table 13.

Table 13. **Status of Sensor Technology in the Glass Industry** <sup>a</sup>

Parameter to be controlled	Related property being measured	Influencing variables	Sensor	References
color	redox analysis Fe/Cr analysis	batch composition organic contamination	sensor based on voltammetry	175, 176
combustion space parameters	glass surface temperature gas temperature gas velocity heat	temperature profile operation parameters	complex sensor based on laser doppler veloci- metry, radia- tion flux probe, pyrometer and gas analysis system	177
corrosion of superstructure	NaOH vapor concentration in combustion chamber	temperature glass melt composition	D <sub>Na</sub> line measurement	178

Table 13 (Continued)

Parameter to be controlled	Related property being measured	Influencing variables	Sensor	References
		location in chamber and turbulence	gas extraction and chemical analysis of aqueous solutions by AA or ICP	179
			gas extraction and <i>in situ</i> analysis of NaOH using Na-sensitive electrodes (similar for KOH)	180
			In situ Na $\beta$ -alumina thermodynamic cell	180
			LIFF (laser-induced fragmentation fluorescence), also proposed to detect KOH	181
			LIBS (laser-induced breakdown spectroscopy), also proposed to measure temperature	182
corrosion of glass-contact refractories	acoustic impedance of refractories	glass composition temperature level	sensor based on ultrasonics and high-temperature piezoelectrics coupled with echo-impact instrumentation	183–188
	dielectric constant of refractories	glass composition temperature level	sensor based microwave (radar) techniques	189–190
fining process	redox state, <i>in situ</i> sulfate analysis	fining agent addition batch redox temperature level	electrochemical measurements using HVG sensor or RAPIDOX sensor	191,192
flame characteristics and combustion parameters	radicals, CO, soot	air/gas or oxygen/fuel ratio fuel input rate	optical sensor based on flame spectra analysis	193

Table 13 (Continued)

Parameter to be controlled	Related property being measured	Influencing variables	Sensor	References
	digital images of flames and optical spectroscopic determinations	air/gas or oxygen/fuel ratio fuel input rate	sensor uses recognition technique is based on computer analysis of the images, proposed to measure NO <sub>x</sub> and it can estimate flame temperature	194
gas bubbles	defect diagnosis by acoustic methods	batch composition fuel input temperature profile burner settings	ultrasonic techniques	195
glass gobs	melt viscosity plunger frequency	temperature feeder plunger settings	sensor based on image analysis	196
homogeneity	refractive index variation	temperature profile in melter forced bubbling electric boosting	Christiansen-Shelyubskii method; computer simulation	197
pressure	combustion chamber pressure	air leakages	available (a commodity product)	
	O <sub>2</sub> partial pressure of Sn in glass float bath	glass surface degradation	Sn/SnO <sub>2</sub> thermodynamic cell	198
temperature	combustion chamber temperature temperature of lining	operation parameters	Pt/Pt-Rh thermocouples (a commodity product)	
	glass melting temperature	operation parameters	"smart" sensor based on coupling a thermocouple with an optical pyrometer	199
viscosity	temperature	heat input glass composition melting history redox of batch	in-line (rotation/vibration) viscometer for feeders	
	electromagnetic radiation	heat input glass composition melting history redox of batch	ceramic waveguide that sends a coherent millimeter-wave signal to the molten glass and the reflection back to the detector	200

<sup>a</sup>Adapted from Ref. 174.

*Computer Modeling of Glass Melting.* Several physical and mathematical modeling techniques are being implemented to investigate glass-making processes, optimize these processes, and evaluate new or different operating conditions, including the following:

- Design new manufacturing installations to reduce costs of plant construction and plant operation while increasing furnace life.
- Investigate and solve day-to-day operation problems.
- Improve process efficiency, fuel efficiency, throughput rates, production yields, and product quality (less defects).
- Develop new products and processes in less time.
- Ensure environmental quality and meet current or projected regulations.

Figure 19 summarizes the mathematical models used in the glass industry (201). This section relates to Process Models, which outputs a product characteristic or a materials parameter, such as glass melt velocity and temperature. Environmental models relate process variables to the emissions from the furnace and can be treated as a subset of the Process Models. Control models relate controllable process variables to the critical process and product variables. One example is the control of burners and emissions by digital analysis of flame images (Table 13). Property models relate glass properties to the composition (ie, databases described in the Properties section). The most sophisticated level include atomistic and molecular modeling relating glass structure to properties (as exposed in the Fundamentals section).

Under Process models, “Black Box” models are semiempirical models used to input more complex models. “Overall Balance” models refer to momentum, heat and mass flow models used to estimate pressure drop, and heat and mass balances in glassmaking. Continuum models refer to the use of continuum mechanics equations to fully describe a given process in glassmaking: Navier-Stokes, differential thermal and species balances, and phenomenological laws describing the relationship between flux and gradients. As the glassmaking process involves several steps (melting, dissolution, glass delivering to forming

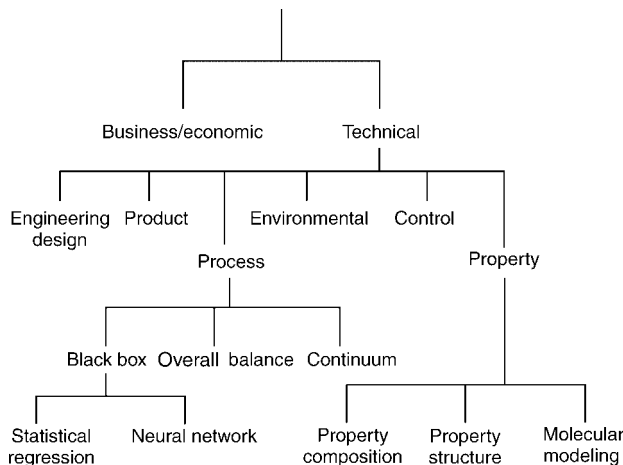


**Fig. 19.** Classification of mathematical models used in the glass industry (201).

machines), an ideal mathematical model would be one that covers the various parts of the process that are then linked into one output. Software has been written especially for modeling 3D flow and heat-transfer phenomena in glass-melting tanks and is commercially available: The Netherlands Organization TNO (202), Glass Service Ltd. (203), and the Instituto Superior Técnico (204). The U.S. DOE is supporting a new effort at the Argonne National Laboratory to develop a Combustion Space and Glass Bath Furnace Simulator which will be provided to the industrial users at no cost and support through a user center (205).

**4.3. Advanced Melting Techniques.** Most manufacturing and glass processing starts by converting raw materials into a homogeneous melt at high temperatures as has been summarized in the sections on Glass Manufacturing Processes and Glass Melting Tanks. Still, other methods have been used to obtain special materials and include obtaining, eg, glass microspheres. Aluminosilicate glass microspheres (Fig. 20) that range in diameter from 1 to  $\sim 100\ \mu\text{m}$  are made by a flame spraying technique. After melting, the glass is crushed to particles of about the desired size. The particles are then passed through a suitable flame where they melt and form spherical droplets due to surface tension (206).

Other methods include sol-gel processing (207–209); vapor deposition for optical waveguides and optical mirrors (210–213), including nanoglass technologies (214); reactive sputtering for many special oxide glasses (ie, Ref. 215); thermal oxidation as in making passivating films of  $\text{SiO}_2$  on silicon (211); and anodic oxidation on a metal or a semiconductor (216).

The following are being reevaluated for advanced melters: submerged combustion melting (a 6 ton/day unit is production in Ukraine) (217), the BOC convective glass melting system (CGM), which directs oxyfuel flames vertically down onto the batch surface at the charging end of the furnace (218,219), Microwave of silicate glasses (220), induction melting (221), and plasma melting (222),

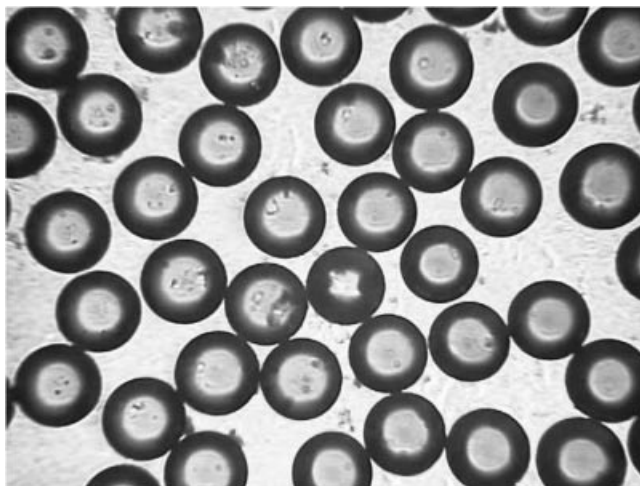


**Fig. 20.** Accuspheres are being produced in closed ranges up to  $100\ \mu\text{m}$ . Courtesy of Prof. Delbert Day, Mo-Sci Corp.

a technique that has been used to melt iron silicates in metal recuperation units (223) and is being used in Japan as waste incinerators 224.

Finally, the U.S. DOE is promoting a program called Next Generation Melter to develop new melting technologies that will significantly increase the efficiency and lower the cost of glass production (225). The first stage was conducted in 2001 and 2002. A review has been made on different methods that have been used, or proposed, to melt glass in industry. These include PPGs P-10 (226) which is a patented melting system and currently used in only one furnace, with no widespread application in the glass industry. The system separates the glass-formation process into four discrete devices to optimize the following elements: (1) raw materials, as a thoroughly mixed batch, are preheated to enhance reaction temperatures  $<540^{\circ}\text{C}$ ; (2) the batch is heated with an oxyfuel flame to a temperature that melts the batch ingredients and promotes the primary solid-state reactions of dissolving the sand and begins the conversion to the glassy state; (3) the molten mixture is held at temperatures to allow evolution of  $\text{CO}_2$  and  $\text{H}_2\text{O}$  from raw materials and allow fluxing reactions to complete the dissolving of more refractory components; and (4) a vacuum is applied to force refining mechanisms to remove remnant seeds.

## 5. Glass Recycling

Glass has lost market share to aluminum and plastics for almost four decades as consumers are purchasing lightweight containers and throwing them away after use. High costs of waste disposal and shrinking landfill suggest that recycling is the appropriate approach for different waste materials (227).

Manufacturers benefit from recycling in several ways; it reduces consumption of raw materials, extends the life of plant equipment such as furnaces and saves energy. Glass container manufacturing is an example of a closed-loop recycling; meaning old bottles and jars can be turned into new containers over and over. This is a significant advantage in marketing this packaging to both the customers of companies and the consumers. All companies are seeking additional quantities of cullet and can use more than is presently being generated. It must

- Meet local plant specifications.
- Be available in consistent quantities.
- Be priced comparably with the raw materials for which it substitutes.

And, as is the case with other raw materials, cullet is subject to quality control standards that take into account its impact on the manufacturing process. This has become increasingly critical as more and more recycling programs are commingling glass and other materials during collection and processing.

## 6. Uses

Glass is commonly used in different applications such as architecture (228), beverage containers, insulation (noise, thermal, eg) and some lesser known

applications such as nuclear waste encapsulation (229). The newer applications of glasses include components in solid-state batteries, electronic switches and memories, electrophotography, solar cells, microspheres for optical strengthening and medical uses, novel glass-ceramics (machinable and bioactive materials), solder and sol-gel glasses, gradient index optics, communication fibers, sensors, and nonlinear, active, and digital optics (230–232).

**6.1. Container, Architecture, Insulation.** Silicate glasses are commonly used in beverage containers, window panes, and automobile windshields. However, coatings are used to obtain properties not inherent in glasses. The most widely used is silver coatings in mirrors. Today, most demand on coatings is on sodalime silica (SLS) glass surfaces and include architectural coatings (to reflect ir wavelengths reducing solar gain, control of light), container coatings (to prevent surface contact damage), and automotive coatings (window defrosters, color enhancement, support for electrical-electronic connections). Recently, coatings have been used in the optical fiber industry, that can strengthen the glass as well as provide lubricity and abrasion resistance (233–234). Other developments are thin-film based products, such as liquid-crystal and electrochromic glazing that provide occupant-adjustable optical properties in automotive applications. Most of these applications demand that the coatings have high abrasion and chemical resistance and adhere strongly to the substrate. Coating research continues to improve cost reduction, coating application, and understanding the role of different treatments. Two general methods are known for preparing SLS substrates to obtain high quality coatings and both depend on an alkali diffusion barrier (235). In the first method, the glass surface is coated with pure  $\text{SiO}_2$  by a sol-gel process. The  $\text{SiO}_2$  coated substrate is heated then at  $500^\circ\text{C}$  where some densification occurs. A second method is gas-phase dealcalization procedure based on the reactions with acidic gases,  $\text{HCl}$ ,  $\text{SO}_2$ ,  $\text{SO}_3$ , and DFE (1,1-difluoroethane). The sol-gel coating provides higher quality  $\text{SnO}_2$  coatings as compared to dealcalized SLS substrates.

*Container Coatings.* This surface treatment lubricates glass containers so they can be handled safely. The main process used is a cold-end coating of polyethylene combined with a hot-end coating of  $\text{SnO}_2$  or  $\text{TiO}_2$ . Lubricity is regulated by varying the amount of polyethylene. Hot-end coatings are applied before annealing, using  $\text{SnCl}_4$  or  $\text{TiCl}_4$  or organic tin compounds by a CVD process to produce coatings of either  $\text{SnO}_2$  or  $\text{TiO}_2$ . Cold-end coatings are organic materials applied after the annealing lehr. Materials for cold-end coatings include polyethylene, oleic acid, stearates, and silicones.

SurShield barrier material is a proprietary formulation, available from Owens-Illinois (236). The material is an active and passive barrier for oxygen, and substantially improves the protection against  $\text{CO}_2$  permeation ( $\text{CO}_2$  permeation varies by container design). The efficiencies of SurShield barrier material can deliver key advantages for lowering total package costs; all while preserving product freshness and extending shelf life.

*Automotive Coatings.* Thin-film glass coatings are used for various purposes: to reduce interior heat build-up and air conditioner load by reflecting solar ir radiation; to provide heat to melt ice and frost from the windshield; to increase reflection and reduce visible transmission for rear occupant privacy; to reduce glare and enhance driver visibility; to serve as radio and telephone antennae;

to provide an enhanced reflective region on the windshield for instrument display; to reduce emissivity to prevent frost build-up; to act as moisture sensors to trigger defrost and wiper operation; and to provide matching colors to enhance styling (237). Some coatings are being used to perform more than one function. An electrically heated windshield that also reduces solar heat load and electrically conductive coatings for heatings, or for solar reduction, may also be used as radio or mobile phone antennae.

Current coating technologies include on-line (a continuous process, integral with the float glass-making process) vs off-line procedures, pyrolytic (vs ambient temperature, vacuum vs ambient pressure, chemical vs physical deposition, before vs after glass bending, and monolithic vs laminated). Pyrolytic and chemical processes were the first to be widely applied to automotive glass and remain the most economical and widely used in terms of area of glass coated per year. Technology for pyrolytic deposition on the float glass ribbon for large scale automotive applications was first introduced by Ford Motor Co. in 1977. The coatings must be able to withstand subsequent high temperature (600°C) bending and temperature operations without degradation.

Off-line processes offer greater flexibility in a batch mode; film chemistry; and the control of important parameters such as temperature, pressure, and glass speed. However, the process must be preceded by thorough washing and drying. Off-line processes are typified by vacuum sputtering. Thick-film coatings are applied off-line by silk screen prior to bending or tempering, high temperature steps that serve to fire the coatings.

*Architectural Coatings.* SPD (suspended particle devices) film allows the production of a “smart” window that provides controllable degrees of light transmission. Used in conjunction with low E glass, which reflects heat and other commercially available materials, SPD smart windows can also block uv light and promote energy efficiency. SPD refers to light-absorbing microscopic particles that are suspended between two conductive-coated surfaces. The film is placed between two panes of electrically conductive-coated glass or plastic. By turning the electrical voltage up or down, the amount of light transmitted through the glass or plastic window can be controlled (238). SPD uses an emulsion that is enhanced by adjusting the composition of the matrix polymer and the liquid suspending medium such that these materials have a refractive index within the range of 1.455–1.463. This adjustment, while maintaining immiscibility, increases the affinity between the matrix and liquid suspending medium. This allows small droplets of the liquid suspending medium to exist for substantially longer periods of time without coalescence.

PPG SunClean Glass (239) is a coated glass product with photocatalytic and hydrophilic properties that combine to make windows easier to maintain. The transparent SunClean coating is applied to hot glass during the forming process, where it forms a strong, durable bond with the glass surface. The photocatalytic property of the coating is triggered by the sun’s uv rays, and works to slowly break down and loosen organic dirt. At the same time, the coating’s hydrophilic property causes water droplets to spread out and sheet over the coating’s surface (Fig. 21). This sheeting action helps to rinse away loosened dirt. The self-cleaning property of the glass is made possible by a durable, transparent coating of titanium dioxide (TiO<sub>2</sub>) applied during the manufacturing process. The application

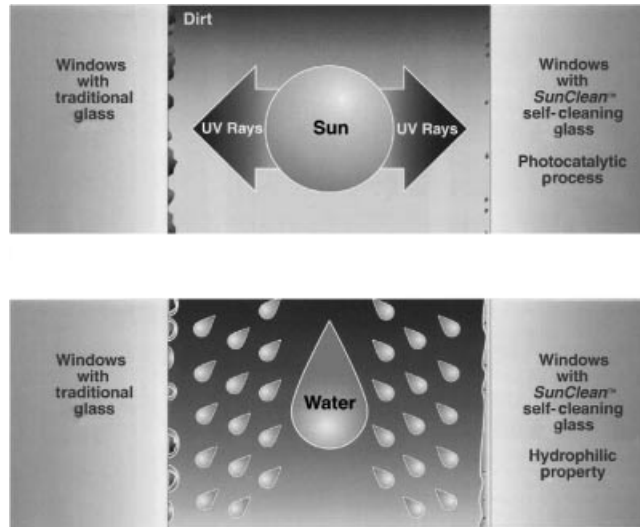


**Fig. 21.** PPGs self-cleaning window glass. Courtesy of PPG Corp.

process, patented by PPG, makes the coating an integral part of the outer glass surface, providing homeowners with a durable, long-lasting product. Table 14 summarizes main architectural developments by PPG. Additionally, an overview of the current state-of-the-art of transparent conducting oxides (TCOs) is given by Ginley (240). The main markets for TCOs are in architectural applications, in particular energy-efficient windows, and flat-panel displays (FPDs). Pyrolyzed

**Table 14. Highlights in PPGs Residential Construction History**

Year	Highlight
1883	The Pittsburgh Plate Glass Company is established in Creighton, Pa
1925	PPG begins mass-producing sheet glass
1938	Herculite tempered glass; several times more shatter resistant than plate glass, is introduced
1945	Twindow double-paned insulating glass is placed on the market
1963	PPG becomes the first U.S. company to manufacture glass using the float process
1983	PPG introduces Sungate 100 low-E glass, the world's first low emissivity glass
1989	Sungate 300 low-E glass is introduced
1989	Azurlite glass is developed, providing a low shading coefficient with high visible light transmittance
1992	Intercept insulating glass spacers are developed
1993	Sungate 500 low-E glass is introduced
1995	Sungate 1000 low-E glass is introduced
1997	Intercept DSE insulating glass technology is launched
1999	75th Intercept licensee obtained from Residential Glass manufacturers
2000	Solarban 60 solar control low-E glass is introduced (formerly Sungate 1000 Low-E)
2001	PPG introduces SunClean self-cleaning glass

fluorine-doped tin oxide is widely used as coatings for preventing radiative heat loss from windows. Indium tin oxide (ITO) is usually used in most FPD applications. The volume of FPDs produced, and hence the volume of TCO (ITO) coatings produced, continues to grow rapidly, with a current market value of over \$U.S.  $15 \times 10^9$ .

**6.2. Medical Applications.** Over the last decade, considerable attention has been directed toward the use of bioactive fixation of implants. Bioactive fixation has been defined as “interfacial bonding of an implant to tissue by the formation of a biologically active HAp layer on the implant surface” (241). Studies of various compositions of bioactive glasses, ceramics and glass–ceramics have established that there are different levels of bioactivity, as measured by rates of bonding to bulk implants or, alternatively the rate of osteoblastic proliferation in the presence of bioactive particulates 242.

A limited number of bioactive glass compositions containing  $\text{SiO}_2\text{--Na}_2\text{O--CaO--P}_2\text{O}_5$  with  $<55\%$   $\text{SiO}_2$  exhibit a high bioactivity index that bond to both bone and soft connective tissues and have been identified as bioglasses (243–244). These materials have been classified as Class A, and are osteoproliferative (enhance osteoblastic activity) as well as osteoconductive (bone growth and bond along the material surface). Materials classified as Class B only exhibit osteoconductivity and examples include dense synthetic HAp and AW/GC.

Studies using a bioactive glass, 45S5, have found it to be osteoproliferative, in that it induced differentiation of osteoblasts and stimulated bone formation both *in vitro* and *in vivo* (245). Moreover, ionic products released by the dissolution of this bioglass *in vitro* for 4 days caused enhanced human osteoblasts proliferation and induced insulin-like growth factor II mRNA expression (246). Elemental analysis of the bioglass–conditioned medium during the experiment showed an 88-fold increase in Si concentration and to a lesser extent, changes in Ca and P concentration relative to the controls. Such a material can be considered ideal for tissue engineering as the released by-products promote desired cellular responses. Table 15 summarizes recent medical and dental technological developments. An overview of recent applications of optical-fiber sensors use has been presented by Baldini (247).

New glass-based materials are being developed to repair bone by mixing crushed glass particles with a polymer. The mixture is to be injected into the area of a crushed vertebrae or other damaged bone that then fills the cracks, gluing the broken pieces back together. Once this mixture hardens, it turns into a bonelike substance, bonding itself to the original bone. Another method is being devised to use biodegradable glass spheres that will be used to irradiate arthritis joints. For example, small radioactive glass spheres, about one-fifth to one-tenth the diameter of a human hair, can be injected into the damaged joint. Once the radiation is delivered, the spheres gradually react with the body fluids and eventually disappear from the body, thus creating a safe way to expose a patient to radiation, confining the entire radioactivity to the diseased joint. Similar procedures can be used to treat other ailments. Instead of using a solid glass sphere, a hollow sphere or shell filled with a drug and injected into the body, or spread as a cream onto the skin and gradually released into the body’s system. This type of treatment releases the drug in a more uniform manner and targets the infection or diseased area (248).

Table 15. Recent U.S. Patents in Medical and Dental Applications

Assignee <sup>a</sup>	Patent no.	Short title
3M	6,437,019	Ionomer cement
US Biomaterials	6,423,343	Bioactive glass
Ivoclar AG	6,420,288	Translucent lithium disilicate glass
Jeneric/Pentron Inc.	6,403,676	Dental composites
Schott Glas	6,403,506	Glass powder
Jeneric/Pentron Inc	6,375,729	Machinable glass–ceramics
Degussa-Huls	6,362,251	Dental material
GC Corporation	6,355,585	Ionomer cement
U. Missouri-Rolla	6,379,648	Biodegradable glass
Ivoclar AG	6,342,458	Dental product
US Biomaterials	6,338,751	Bioactive glass
TDK Corp.	6,306,785	Living tissue replacement
Ivoclar AG	6,306,784	Alkali silicate glass
U. of Pennsylvania	6,303,290	Porous glass-like matrices
Schott Glas	6,297,181	Barium-free X-ray-opaque dental glass
Ivoclar AG	6,280,863	Translucent apatite glass ceramic
Schott Glas	6,278,896	Biocompatible glass-metal
U. of Maryland	6,244,871	Bioactive glass compositions
NA	6,224,662	Dental glass pillars
Ivoclar AG	6,200,137	Chemically stable translucent apatite glass ceramic
NA	6,255,477	Magnetic glass for separating biological material
NA	6,197,342	Biologically active glass as a drug delivery system
U. of Florida	6,190,684	Injectable bioactive glass in a dextran suspension

<sup>a</sup>NA = none designated.

Liver cancer is being treated today with rare earth aluminosilicate (REAS) glass microspheres. These glasses are free of alkali oxides so their chemical durability is extremely high. The interest in REAS glasses stemmed from the need to deliver a radioactive material into a diseased organ instead of external beam radiation. By irradiating the organ *in situ*, shorter range  $\beta$  radiation can be used minimizing damage to adjacent healthy tissue. REAS glasses satisfy body requirements such as nontoxic, chemically insoluble in body fluids during treatment, and have specific radioactivity for therapeutic doses. Treatment with radioactive YAS (yttrium aluminosilicate) glass microspheres, TheraSphere (Fig. 22), containing  $\beta$  emitting Y-90, has proven to be a safe method of delivering radiation doses which are five to seven times larger than doses from other methods irradiating the liver.

**6.3. Communication and Electronics.** There are several advantages in using light pulses through silica glass fibers for telecommunications in comparison to copper wires that require repeaters or signal boosters at intervals of  $\sim 2$  km; eg, the repeaters in commercial fiber-optic systems are 30 km apart. Also, the glass fibers are small (typically  $\sim 100$   $\mu\text{m}$ ) and more of them fit into a cable of a given size. The glass fibers are not susceptible to electromagnetic interference, so the signal is clearer. Finally, the information carried on optical fibers can be modulated at very high frequencies with more simultaneous transmissions being possible. Although the standard wavelength of transmission used in silica optical fiber networks is in the ir ( $1.55$   $\mu\text{m}$ ), there are applications in

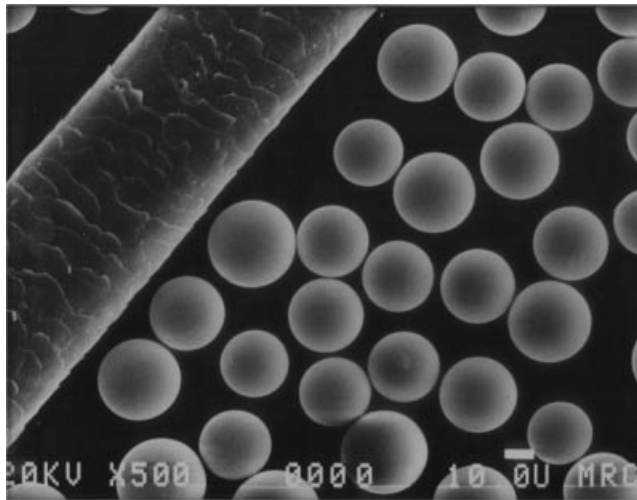


**Fig. 22.** TheraSphere, microspheres smaller than a human hair (1–100  $\mu\text{m}$ ) made from rare earth aluminosilicate glasses to deliver large doses of beta radiation to diseased body organs. Courtesy of Prof. Delbert Day and Mo-Sci Corporation.

which glasses transmitting to longer wavelengths are preferable. These include nose cones for heat-seeking missiles; noninvasive monitoring of bodily fluids, eg, analysis of blood by transmitting ir radiation through an earlobe; and lenses for night vision equipment. Some chalcogenide and halide glasses transmit to the far-ir region (up to  $\sim 20 \mu\text{m}$ ).

Light-focusing glass fibers and rods having radially parabolic refractive index distributions are known as graded-refractive index (GRIN) devices (249,250). GRIN glasses are used as waveguides for coupling optical fibers and as lenses for compact photocopiers and compact disk players. The use of graded-refractive index lenses could also reduce the number of elements needed in complicated optical systems such as cameras and microscopes.

Other glasses, fluorozirconate glasses, for instance, transmit into the mid-ir, and may be suitable for applications requiring relatively short lengths of fiber. Tables 16 and 17 summarize recent technological developments regarding optical applications and electronic applications, respectively.

**Photonic Applications.** Optoelectronic applications such as optical switches and modulators require materials having NLO properties; eg, the refractive indexes are nonlinear dependent on the intensity of the applied electric field and are noticeable only high energy sources such as lasers are used. It has been found that glasses containing small amounts of semiconducting microcrystals exhibit large optical nonlinearities (251,252). Halides and chalcogenide glasses present potential applications in infrared optics and optoelectronics (253).

Many organic and inorganic solids have been considered for photonic applications because of their nonlinear optical properties. Chalcogenide glasses with nonlinear refractive index have been theoretically identified to be some such candidate materials (254,255). Another new family of glasses with high nonlinear

Table 16. Recent U.S. Patents in Optical Applications

Assignee <sup>a</sup>	Patent no.	Short title
Heraeus Quarzglas GmbH	6,451,719	Silica glass for excimer laser
Sumitomo Electric Physical Optics Corp.	6,449,986	Porous glass for optical fiber
Asahi Glass Co.	6,446,467	Monolithic glass light shaping diffuser
Shin-Etsu Chemical Co. Ltd.	6,451,434	Glass laminate, functional transparent article
Shin-Etsu Chemical Co. Ltd.	6,442,978	Apparatus for sintering a porous glass
Corning Inc.	6,441,549	Glass envelope with continuous internal channels
Matsushita Electric Industrial	6,439,943	Plasma display panel
Hoya Corp.	6,434,976	Glass fiber
Philips Electronics N. A.	6,433,471	Plasma addressed liquid-crystal display with glass spacers
Nikon Corp.	6,432,854	Polarizing optical system
Inst. of Phys. and Chem. Research NA	6,432,278	Controlling refractive index of silica glass
Corning Inc.	6,431,935	Lost glass process used in making display
Schott ML GmbH	6,429,162	Glass for high and flat gain 1.55 $\mu$ optical amplifiers
Corning Inc.	6,423,656	Synthetic quartz glass preform
Corning Inc.	6,418,757	Method of making a glass preform
Fitel USA Corp.	6,416,235	Glass ferrule optical fiber connectors
Alcatel	6,412,310	Gravity feeding powder to a plasma torch
Shin-Etsu Chemical Co.	6,413,682	Quartz glass substrate for photomask
Electron. Telecom. Res. Inst.	6,413,891	Glass material for waveguide of an optical amplifier
Hoya Corp.	6,413,894	Optical glass and optical product
Corning Inc.	6,410,467	Antimony oxide glass with optical activity
Tosoh Corp.	6,405,563	Opaque silica glass with transparent portion
Nikon Corp.	6,378,340	Synthetic silica glass
NA	6,374,641	Optical fiber by melting particulate glass in a glass cladding tube
Sumita Optical Glass, Inc.	6,372,155	Oxide glass with long afterglow and accelerated phosphorescence
Corning Inc.	6,362,118	Negative thermal expansion optical waveguide substrate
Corning Inc.	6,360,564	Sol-gel method of preparing powder for use in forming glass
NTT Corp.	6,356,387	Tellurite glass optical amplifier
Schott Glas	6,353,284	Glass funnel for television tube
None	6,352,949	Fluoro glass ceramic
Olympus Optical Co.	6,342,460	Infrared absorbing glass

<sup>a</sup>NA = none designated.

optical properties, so-called quantum dot solids, is formed by nanocomposites made up with microcrystallites of cadmium sulfide and cadmium selenide in a silicate glass matrix. Various groups in the world are engaged in the preparation of such nanocomposites via the sol-gel method (256).

**Optical Fiber Sensors.** Advances in optical-fiber temperature and pressure sensors have been reviewed by Grattan (257) highlighting industrial applications of fiber-optic temperature sensors. Temperature sensing is limited by the

Table 17. Recent U.S. Patents in Electronic Applications

Assignee	Pat. no.	Title
Schott Glas	6,417,124	Alkali-free aluminoborosilicate glass and uses
Hoya Corp.	6,442,975	Thin-plate glass article for information recording medium
Hitachi Ltd.	6,440,517	Glass material
Sumitomo Electric Industries	6,438,997	Method of elongating glass preform
IBM	6,436,332	Low loss glass-ceramic composition with modifiable dielectric constant
Hoya Corp.	6,430,965	Glass substrate for information recording medium
Ohara KK	6,426,311	Glass-ceramics for substrates
Schott Glas	6,420,291	Lead silicate glass and a process for setting a reduced surface resistance
Murata Manufacturing Co.	6,414,247	Glass ceramic board
Nippon Electric Glass	6,413,906	$\text{Li}_2\text{O}-\text{Al}_2\text{O}_3-\text{SiO}_2$ crystallized glass
Nippon Sheet Glass Co.	6,413,892	Glass substrate for magnetic recording media
Samsung Electronics	6,410,631	Composition for production of silica glass using sol-gel process
Sanyo Electric Co.	6,400,438	Glass board used in the production of liquid-crystal panels
Hitachi, Ltd.	6,384,347	Glass-ceramic wiring board
None	6,381,986	Sintered quartz glass products
Tyco Electronic Corp.	6,379,785	Glass-coated substrates for high frequency applications
Schott Glas	6,376,402	Glasses and Glass-ceramics with high specific Young's modulus
US Navy	6,376,096	Nanochannel glass replica membranes
Nippon Sheet Glass	6,376,084	Glass-ceramics substrate for information recording medium
Asahi Glass Co.	6,362,119	Barium borosilicate glass and glass-ceramic composition
Fujitsu Ltd.	6,361,867	Laminated glass substrate structure
None	6,355,587	Quartz glass products and methods for making
Nippon Sheet Glass	6,355,353	Glass substrate having transparent conductive film
Agfa-Gevaert	6,355,125	Electric or electronic module comprising a glass laminate
Kyocera Corp.	6,348,427	High-thermal expansion glass-ceramic sintered product
NEC Corp.	6,348,424	Low temperature calcined glass-ceramic and manufacturing process
NEC Corp.	6,344,424	Low melting point glass, insulating package, and sealing member
Nikon Corp.	6,339,033	Silica glass having superior durability against excimer laser beams
Murata Manufacturing Co.	6,335,298	Insulating glass paste and thick-film circuit component

maximum service temperature of the fibers. Advanced temperature and pressure sensors are based on Bragg gratings. Optical-fiber sensors based on fiber Bragg gratings (FBGs) provide accurate, nonintrusive, and reliable remote measurements of temperature, strain, and pressure, and they are immune to

electromagnetic interference. FBGs are extensively used in telecommunications, and as sensors, FBGs find many industrial applications in composite structures used in the civil engineering, aeronautics, train transportation, space, and naval sectors. Tiny FBG sensors embedded in a composite material can provide *in situ* information about polymer curing (strain, temperature, refractive index) in a nonintrusive way. Additionally, FBGs may be used in instrumentation as composite extensometers primarily in civil engineering applications (258,259).

**6.4. NIF Laser Glass.** The National Ignition Facility (NIF) (260) has both the largest laser and the largest optical instrument ever built. The NIF laser system uses ~3100 large plates (3-ft long and about one-half as wide) of an neodymium phosphate glass manufactured (Hoya Corporation, USA and Schott Glass Technologies, Inc.). The main objective of the NIF optics is to steer 192 laser beams through a 700-ft long building onto a dime-size laser-fusion target, compressing and heating BB-sized capsules of fusion fuel to thermonuclear ignition. NIF experiments will produce temperatures and densities like those in the Sun or in an exploding nuclear weapon. The experiments will help scientists sustain confidence in the nuclear weapon stockpile without nuclear tests. It will also produce additional benefits in basic science and fusion energy.

**6.5. Glasses for Nuclear Waste Disposal.** Vitrification is being used to immobilize high level nuclear waste (HLW) in a stable, chemically durable borosilicate glass (261–266). In the waste vitrification process, the glass melt is contained in a refractory-lined furnace. The high-temperature melt dissolves the HLW but also corrodes the refractory. Knowledge of the corrosion resistance of refractories to melts containing HLW is of considerable importance to the vitrification technology (267).

The borosilicate glass is being used to vitrify HLW at the Savannah River Site in Aiken, S.C., and by West Valley Nuclear Services at West Valley, N.Y. (268,269). Borosilicate glasses have a good chemical durability, but may not be suitable for all HLW compositions, such as, wastes containing phosphates, halides and heavy metals (Bi, U, Pu).

Many phosphate glasses have a chemical durability that is usually inferior to that of most silicate and borosilicate glasses, but iron phosphate glasses are an exception (270). In addition to their generally excellent chemical durability, iron phosphate glasses have low melting temperature, typically between 950 and 1150°C (271). Investigations of iron phosphate wasteforms obtained by adding different amounts of various simulated nuclear wastes to a base iron phosphate glass, whose composition is 40Fe<sub>2</sub>O<sub>3</sub>–60P<sub>2</sub>O<sub>5</sub> (mol %) showed that these glassy wasteforms have a corrosion rate up to 1000 times lower than that of a comparable borosilicate glass (272–274). Generally, iron phosphate glasses can contain up to 40 wt% of certain simulated waste. Because of their unusually high chemical durability and other properties, ironphosphate glasses, zinc–iron phosphate glasses (275), and lead–iron phosphate glasses are of interest for nuclear waste immobilization. The composition of high level nuclear wastes (HLW) at Hanford from tank B-110 is shown in Table 18. The B-110 waste comes from different steps in the bismuth phosphate process which accounts for the high concentration of Bi<sub>2</sub>O<sub>3</sub> (276).

Table 18. Simplified Composition of Hanford B-110 Waste and Raw Materials Used to Prepare Simulated B-110 Waste<sup>a</sup>

Compound	B-110, wt%	Raw materials used
Fe <sub>2</sub> O <sub>3</sub>	30.6	Fe <sub>2</sub> O <sub>3</sub>
P <sub>2</sub> O <sub>5</sub>	1.7	NH <sub>4</sub> H <sub>2</sub> PO <sub>4</sub>
Bi <sub>2</sub> O <sub>3</sub>	25.8	Bi <sub>2</sub> O <sub>3</sub>
SiO <sub>2</sub>	23.4	SiO <sub>2</sub>
Na <sub>2</sub> O	14.4	Na <sub>2</sub> CO <sub>3</sub>
Al <sub>2</sub> O <sub>3</sub>	2.7	Al <sub>2</sub> O <sub>3</sub>
CaO	1.5	CaCO <sub>3</sub>

<sup>a</sup>Ref. 270.

**6.6. Economic Future of Glass in Construction Business.** Hundreds of private companies are active in the  $\$13.7 \times 10^9$  U.S. flat and other fabricated glass industry (eg, Cardinal IG, Fenton Art Glass, Guardian Industries, Safelite Glass, Schott, United Glass) (277). Demand for flat glass in the United States will approach  $7 \times 10^9$  ft<sup>2</sup> in 2005. Rebounding automobile production will boost demand for laminated and tempered glass, while high energy costs and standards benefit insulating glass in the repair–improvement construction segment. World demand for flat glass will approach  $4 \times 10^9$  m<sup>2</sup> in 2004, valued at U.S.  $\$40 \times 10^9$  (Asahi Glass, Pilkington, Saint-Gobain, Guardian Industries, PPG Industries, Nippon Sheet Glass, Visteon, Vitro, Apogee Enterprises, and Donnelly). Construction markets will grow the fastest based on expanding global fixed investment.

U.S. lighting fixtures (U.S.  $\$16.7 \times 10^9$  electric lighting fixtures industry) demand will grow 4.8% yearly through 2006, driven by continued strength in replacement markets where efficiency concerns generate remodeling and retrofit projects. High efficiency products will lead gains, including electronic ballasts, high intensity discharge (HID) lighting, light emitting diodes (LEDs) and fiber optic systems.

Demand for glass fibers (U.S.  $\$5.4 \times 10^9$  glass fiber industry, 39 key companies including Owens Corning, Johns Manville, Saint Gobain, and PPG Industries) in the United States will reach  $6.8 \times 10^9$  lb in 2005. The best opportunities are expected for textile glass in reinforced plastics applications based on advantages over competitive materials (eg, light weight, corrosion resistance, and favorable cost–performance profile).

## BIBLIOGRAPHY

“Glass” in *ECT* 1st ed., Vol. 7, pp. 175–206, by H. G. Vogt, Corning Glass Works; in *ECT* 1st ed., Suppl. 2, pp. 435–454, by S. D. Stookey, Corning Glass Works; in *ECT* 2nd ed., Vol. 10, pp. 533–604, by J. R. Hutchins III and R. V. Harrington, Corning Glass Works; in *ECT* 3rd ed., Vol. 11, pp. 807–880, by D. C. Boyd and D. A. Thompson, Corning Glass Works; in *ECT* 4th ed., Vol. 12, pp. 555–627, by D. C. Boyd, P. Danielson, and R. K. Brown, Corning Inc.; “Glass” in *ECT* (online), posting date: December 4, 2000, by David C. Boyd, Paul S. Danielson, David A. Thompson, Corning Incorporated.

1. G. W. Morey, *The Properties of Glass*, 2nd ed., Reinhold Publishing Corp., New York, 1954, p. 28.
2. ASTM C162-99, *Standard Terminology of Glass and Glass Products*, 1999.
3. J. E. Shelby, *Introduction to Glass Science and Technology*, RSC Paperbacks, The Royal Society of Chemistry, 1997.
4. D. R. Uhlmann, *J. Phys. C* **9**, 175 (1982).
5. N. J. Kreidl and A. Angell, in D. R. Uhlmann and N. J. Kreidl, eds., *Glass: Science and Technology*, Vol. 1, Academic Press, Boston, Mass., 1983, p. 49.
6. V. M. Goldschmidt, *Akd. Skr. Oslo* **8**, 137 (1926).
7. W. H. Zachariasen, *J. Am. Chem. Soc.* **54**, 3841 (1932).
8. B. E. Warren, *J. Am. Ceram. Soc.* **17**(8), 249 (1934).
9. A. C. Wright, *J. Non-Cryst. Solids* **106**, 1 (1988).
10. W. D. Kingery, H. K. Bowen, and D. R. Uhlmann, *Introduction to Ceramics*, 2nd ed., John Wiley & Sons, Inc., New York, 1976, Chapt. 3.
11. B. E. Warren and J. Bischof, *J. Am. Ceram. Soc.* **21**, 49 (1938).
12. G. N. Greaves, in C. R. Catlow, ed., *Defects and Disorder in Crystalline and Amorphous Solids*, Kluwer Academic, Dordrecht, 1994, p. 87.
13. X. Yuan and A. N. Cormack, *Mater. Res. Soc. Symp. Proc.* **455**, 242 (1997).
14. G. N. Greaves, *J. Non-Cryst. Solids* **71**, 203 (1985).
15. D. A. McKeon, G. A. Waychunas, and G. E. Brown, *J. Non-Cryst. Solids* **74**, 325 (1985).
16. H. Inoue and I. Yasui, *Phys. Chem. Glasses* **28**, 63 (1987).
17. Ref. 3, p. 79.
18. D. R. Uhlmann and A. G. Kolbeck, *Phys. Chem. Glasses* **17**, 146 (1976).
19. D. L. Griscom, in L. D. Pye, V. D. Frechette, and N. J. Kreidl, eds., *Borate Glasses: Structure, Properties, Applications*, Plenum, New York, 1978, p. 11.
20. M. Velez and R. Fernandez, *Acta Cient. Ven.* **46**, 232 (1995).
21. J. Swenson and L. Borjesson, *Phys. Rev.* **B55**, 1138 (1997).
22. J. W. Zwanziger, *J. Non-Cryst. Solids* **192-193**, 157 (1995).
23. P. J. Bray, J. F. Emerson, D. Lee, S. A. Feller, D. L. Bain, and D. A. Feil, *J. Non-Cryst. Solids* **129**, 240 (1991).
24. E. I. Kamitos and G. D. Chryssikos, *J. Mol. Struct.* **247**, 1 (1991).
25. A. C. Hannon, D. I. Grimley, R. A. Hulme, A. C. Wright, and R. N. Sinclair, *J. Non-Cryst. Solids* **177**, 229 (1994).
26. B. Park and A. N. Cormack, *Mater. Res. Soc. Symp. Proc.* **455**, 259 (1997).
27. I. A. Shkrob, M. Boris Tadjikov, and A. D. Trifunac, *J. Non-Cryst. Solids* **262**, 8 (2000).
28. P. J. Bray, *J. Non-Cryst. Solids* **95**, 45 (1987).
29. T. Kanazawa, *J. Non-Cryst. Solids* **52**, 187 (1982).
30. R. K. Brow, C. A. Click and T. M. Alam, *J. Non-Cryst. Solids* **274**, 9 (2000).
31. M. G. Mesko and D. E. Day, *J. Non-Cryst. Solids* **273**, 27 (1999).
32. J. R. Van Wazer, *Phosphorus and its Compounds*, Vol. 1, Interscience, New York, 1958.
33. J. J. Hudgens, "The Structure and Properties of Anhydrous, Alkali Ultra-Phosphate Glasses," Ph.D. dissertation, Iowa State University, Ames, 1994.
34. J. J. Hudgens and S. W. Martin, *J. Am. Ceram. Soc.* **76**, 1691 (1992).
35. R. K. Brow, D. R. Tallant, S. T. Myers, and C. C. Phifer, *J. Non-Cryst. Solids* **191**, 45 (1995).
36. U. Hoppe, G. Walter, R. Kranold, D. Stachel, and A. Barz, *J. Non-Cryst. Solids* **192-193**, 28 (1995).
37. A. Mekki, D. Holland, Kh. A. Ziq, and C. F. McConville, *J. Non-Cryst. Solids* **272**, 179 (2000).

38. Ref. 3, p. 96.
39. D. L. Price and M. L. Saboungi, *Phys. Rev. Lett.* **15**, 3207 (1998).
40. J. Neufeind and K. D. Liss, *Ber. Bunsen. Phys. Chem.* **100**, 1341 (1996).
41. R. Hussim and R. Dupree, D. Holland, *J. Non-Cryst. Solids* **262**, 159 (1999).
42. D. J. Durban and G. H. Wolf, *Phys. Rev.* **B43**, 2355 (1991).
43. X. Lu, H. Jain, and W. C. Huang, *Phys. Chem. Glasses* **37**(5), 201 (1996).
44. A. K. Varshneya, *J. Non-Cryst. Solids* **273**, 1 (2000).
45. M. F. Thorpe, *J. Non-Cryst. Solids* **57**, 355 (1985).
46. A. N. Sreeram, D. W. Swiler, A. K. Varshneya, *J. Non-Cryst. Solids* **127**, 287 (1991).
47. M. Tatsumisago, B. L. Halfpap, J. L. Green, S. M. Lindsay, and C. A. Angell, *Phys. Rev. Lett.* **64**(13), 1549 (1990).
48. M. Poulains, *J. Non-Cryst. Solids* **184**, 103 (1995).
49. R. S. Quimby, in I. Aggarwal and G. Lu, Eds., *Fluoride Glass Fiber Optics*, Academic Press, New York, 1991, p. 351.
50. T. Miyahita and T. Manabe, *J. Quantum Electron.* **QE-18**, 1432 (1982).
51. M. Poulains, *J. Non-Cryst. Solids* **56**, 1 (1983).
52. R. W. Cahn, P. Haasen, and E. J. Kramer, *Materials Science and Technology*, Vol. 9, VCH Publishers Inc, New York, 1991, p. 322.
53. Ref. 19, p. 105.
54. I. Alig, D. Brawn, R. Langendorf, H. O. Wirth, M. Voigt, and J. H. Wendorff, *J. Mater. Chem.* **8**, 847 (1988).
55. C. C. Wu, W. Y. Hung, T. L. Liu, L. Z. Zhang, and T. Y. Luh, *J. Appl. Phys.* **93**, 5465 (2003).
56. H. M. Wu, Y. L. Song, Y. Q. Wen, T. Zhao, H. J. Gao, and L. Jiang, *Prog. Nat. Sci.* **13**, 247 (2003).
57. M. Brewis, G. J. Clarkson, A. M. Holder, and N. B. McClean, *J. Chem. Soc., Chem. Commun.* **12**, 969 (1988).
58. K. Moriwaki, M. Kusumoto, K. Akamatsu, H. Nakano, and Y. Shirota, *J. Mater. Chem.* **8**, 2671 (1988).
59. B. C. Giessen and C. N. J. Wagner, in S. Z. Beer, ed., *Liquid Metals, Chemistry and Physics*, Marcel Dekker, New York, 1972, p. 663.
60. H. A. Davies, *Phys. Chem. Glasses* **17**, 159 (1976).
61. T. E. Sharon and C. C. Tsuei, *Phys. Rev.* **B5**, 1047 (1972).
62. A. Inoue, K. Ohtera, K. Kita, and T. Masumoto, *Jpn. J. Appl. Phys.* **27**, 2248 (1988).
63. A. Inoue, T. Zhang, and T. Masumoto, *Mater. Trans. JIM* **32**, 965 (1991).
64. A. Inoue, *Zurich: Trans Tech.* **1**, 36 (1998).
65. A. Peker and W. L. Johnson, *Appl. Phys. Lett.* **63**(17), 2342 (1993).
66. C. J. Gilbert, R. O. Ritchie, and W. L. Johnson, *Appl. Phys. Lett.* **71**(4), 476 (1997).
67. O. N. Senkov and D. B. Miracle, *J. Non-Cryst. Solids* **317**, 34 (2003).
68. G. He, W. Loser, and J. Eckert, *Scripta Mater.* **48**, 1531 (2003).
69. T. Egami, *J. Non-Cryst. Solids* **317**, 30 (2003).
70. G. Shao, *Intermetallics* **11**, 313 (2003).
71. K. M. Flores, D. Suh, R. Howell, P. Asoka-Kumar, P. A. Sterne, and R. H. Dauskardt, *Mater. Trans.* **42**, 619 (2001).
72. S. J. Pang, T. Zhang, K. Asami, and A. Inoue, *Acta Mater.* **50**, 489 (2002).
73. A. Inoue, T. Zhang, and T. Takeuchi, *Appl. Phys. Lett.* **71**, 464 (1997).
74. T. D. Shen and R. B. Schwarz, *Acta Mater.* **49**, 837 (2001).
75. A. N. Cormack, *The Glass Researcher* **9**, 3 (1999).
76. B. Vessal, A. C. Wright, and A. C. Hannon, in J. H. Simmons, E. R. Fuller, A. L. Dragoo, and E. J. Garboczi, eds., *Proceedings of the Symposium on Computational Modeling of Materials and Processing, Ceram. Trans.*, Vol. 69, The American Ceramic Society Inc., Cincinnati, 1995, p. 27.

77. A. N. Cormack and B. Park, *Phys. Chem. Glasses* **41**, 272 (2000).
78. A. Takada, *Proceedings the XVIII International Congress on Glass*, p. 16.
79. J-J. Liang, R. T. Cygan, and T. M. Alam, *J. Non-Cryst. Solids* **263–264**, 167 (2000).
80. J-F. Poggemann, A. Goss, G. Heide, E. Radlein, and G. H. Frischat, *J. Non-Cryst. Solids* **281**, 221 (2001).
81. W. Panhosrt, in M. Weinberg, ed., *Nucleation and Crystallization in Glass and Liquids*, The American Ceramic Society, Westerville, Ohio, 1993, p. 267.
82. P. Wizinowich, T. Mast J. Nelson, and M. Divittorio, *SPIE* **2199**, 94 (1994).
83. G. H. Beall and L. R. Pinckney, *J. Am. Ceram. Soc.* **82**(1), 5 (1999).
84. W. Panhosrt, *J. Non-Cryst. Solids* **219**, 198 (1997).
85. W. Höland and G. H. Beall, *Glass Ceramic Technology*, American Ceramic Society, Westerville, Ohio, 2002, p. 1.
86. G. H. Beall, in L. L. Hench and S. W. Friedman, eds., *Nucleation and Crystallization in Glasses*, American Ceramic Society, Westerville, Ohio, 1972, p. 251.
87. T. Zhang and T. Masumoto, *J. Non-Cryst. Solids* **473**, 156 (1993).
88. Y. Li, *Scripta Mater.* **36**, 783 (1997).
89. R. Muller, E. D. Zanotto, and V. M. Fokin, *J. Non-Cryst. Solids* **274**, 208 (2000).
90. W. Vogel, *Chemistry of Glasses*, The American Ceramic Society, 1985, p. 111.
91. "Importance of Glass Surfaces to the Glassmaking Industry," *The Glass Researcher*, Vol. **9**(1), 1999.
92. "Surfaces II: Application of Surface Analysis Techniques", *The Glass Researcher*, Vol. **9**(2), 1999.
93. P. H. Gaskell, *J. Non-Cryst. Solids* **222**, 1 (1997).
94. O. V. Mazurin, M. V. Strel'tsina, and T. P. Schvaiko-Schvaikonskaya, *Handbook of Glass Data*, Elsevier, Amsterdam, The Netherlands, 1983.
95. M. B. Volf, *Technical Glasses*, Pitman, London, 1961.
96. SciGlass 3.5 (2001), <http://www.esm-software.com/sciglass/>.
97. Interglad Ver. 5 (2001), [ww7.big.or.jp/~cgi19786/ngf/interglad5/index\\_e.html](http://ww7.big.or.jp/~cgi19786/ngf/interglad5/index_e.html)
98. T. P. Seward, *Ceram. Eng. Sci. Proc.* **22**, 149 (2001); <http://www.oit.doe.gov/glass/factsheets/modeling.pdf>
99. P. Danielson, *The Glass Researcher* **4**, 4 (1995).
100. S. Fujino, H. Takebe, and K. J. Morinaga, *J. Am. Ceram. Soc.* **78**, 1179 (1995).
101. U.S. Pat. 5,668,067 (Sept. 1997), R. J. Araujo, N. F. Borrelli, C. L. Hoaglin, and C. Smith, (to Corning Inc.).
102. U.S. Pat. 5,518,970 (May 24, 1995), P. F. McMillan, C. A. Angell, T. Grande, and J. R. Holloway, (to Arizona State University).
103. W. A. Weyl, *Colored Glasses*, Society of Glass Technology, Sheffield, U.K., 1951.
104. C. R. Bamford, *Color Generation and Control in Glass*, Elsevier, Amsterdam, The Netherlands, 1977.
105. I. Fanderlik, *Optical Properties of Glass*, Elsevier, Amsterdam, The Netherlands, 1983.
106. M. J. Weber, *J. Non-Cryst. Solids* **47**, 117 (1982).
107. R. J. Araujo, *J. Non-Cryst. Solids* **47**, 69 (1982).
108. E. J. Hornyak, *The Glass Researcher* **3**, 10 (1993).
109. A. A. Ahmed, N. A. Ramadan, and I. M. Youssof, *Glass Technol.* **36**(2), 54 (1995).
110. O. Daruelle, O. Spalla, P. Barboux, J. Lambard, and E. Vernaz, *Key Eng. Mater.* **132–136**, 2240 (1997).
111. C. L. Wickert, A. E. Vieira, J. A. Dehne, X. Wang, D. M. Wilder, and A. Barkatt, *Phys. Chem. Glasses* **40**(3) 157 (1999).
112. D. M. Sanders and L. L. Hench, *Am. Ceram. Soc. Bull.* **52**, 662 (1973).
113. M. J. N. Pourbaix, *Atlas of Electrochemical Equilibria*, Pergamon Press, Oxford.

114. R. G. Newton and A. Paul, *Glass Technol.* **21**, 307 (1980).
115. C. J. Brinker and L. C. Klein, *Phys. Chem. Glasses* **21**, 141 (1980); **22**, 23 (1981).
116. M. Velez, D. R. Uhlmann and H. L. Tuller, *J. LatinAm. Met. Mat.* **2**, 3 (1982).
117. M. D. Noirot, *Am. Ceram. Soc. Bull.* **78**, 79 (1999).
118. B. C. Brinker, G. W. Arnold, and J. A. Wilder, *J. Non-Cryst. Solid* **64**, 291 (1984).
119. G. K. Marasinghe, M. Karabulut, C. S. Ray, and D. E. Day, *J. Non-Cryst. Solids* **263–264**, 146 (2000).
120. M. Karabulut, G. K. Marasinghe, P. G. Allen, C. H. Booth, and M. Grimsditch, *J. Mater. Res.* **15**, 1972 (2000).
121. S. T. Reis, M. Karabulut, and D. E. Day, *J. Non-Cryst. Solids* **292**, 150 (2001).
122. D. E. Day, Z. Wu, C. S. Ray, and P. Hrma, *J. Non-Cryst. Solids* **241**, 1 (1998).
123. D. R. Uhlmann, H. L. Tuller, D. P. Button, and M. Velez, *Wis. Z. Friedrich-Schiller Univ. Jena, Math. Naturwiss. R.* **32**, 285 (1983).
124. F. Desanglois, C. Follet-Houttemane, and J-C. Boivin, *J. Mater. Chem.* **10**, 1673 (2000).
125. M. Tatsumisago and T. Minami, *Ceram. Jpn.* **29**, 499 (1994).
126. T. Okura, M. Tanaka, H. Monma, K. Yamashita, and G. Sudoh, *J. Ceram. Soc. Jpn.* **111**, 257 (2003).
127. A. E. Burns, M. Royle, and S. W. Martin, *J. Non-Cryst. Solids* **262**, 252 (2000).
128. T. V. Dubovik, V. Ya. Sushcheva, G. N. Shmat'ko, and L. I. Maikova, *Glass Ceram.* **48**, 350 (1991).
129. P. Znasik, L. Sasek, and M. Rada, *Ceramics-Silikaty* **35**, 33 (1991).
130. M. Yamashita and R. Terai, *Glastech. Ber.* **63**, 13 (1990).
131. C. Tomasi, P. Mustarelli, A. Magistris, and A. I. G. M. Pilar, *J. Non-Cryst. Solids* **293–295**, 785 (2001).
132. C. Wang, M. Nogami, and Y. Abe, *J. Sol-Gel Sci. Technol.* **14**(3), 273 (1999).
133. M. Nogami and K. Yamamoto, *Ceram. Jpn.* **33**, 990 (1998).
134. S. Rossignol, J. M. Reau, B. Tanguy, J. Portier, and J. J. Videau, *Mater. Lett.* **20**, 369 (1994).
135. D. E. Day, *J. Non-Cryst. Solids* **21**, 343 (1976).
136. R. Chen, Yang, B. Durand, A. Pradel, and M. Ribes, *Solid State Ionics* **53–56**, 1194 (1992).
137. A. Bunde, M. D. Ingram, P. Maas, and K. L. Ngai, *J. Non-Cryst. Solids* **131–133**, 1109 (1991).
138. A. Mogus-Milanlikic, B. Santic, D. E. Day, and C. S. Ray, *J. Non-Cryst. Solids* **283**, 119 (2001).
139. *ASTM C 338 Standard Test Method for Softening Point of Glass*, Nov. 15, 1993.
140. *ASTM C 965 Standard Practice for Measuring Viscosity of Glass above the Softening Point*, Oct. 10, 1996.
141. *ASTM C 1036 Standard Test Method for Measurement of Viscosity of Glass between Softening Point and Annealing Range by Beam Bending*, Oct. 10, 1996.
142. *ASTM C 1351M Standard Test Method for Measurement of Viscosity of Glass between 104 Pa.s and 108 Pa.s by Viscous Compression of a Solid Cylinder*, Oct. 10, 1996.
143. N. Leventis, I. A. Elder, D. R. Rolison, M. L. Anderson, and C. I. Merzbacher, *Chem. Mater.* **11**, 2837 (1999).
144. C. R. Kurkjian and U. C. Paek, *Appl. Phys. Lett.* **42**, 251 (1983).
145. M. Koide, R. Sato, T. Komatsu, and K. Matusita, *J. Non-Cryst. Solids* **177**, 427 (1994).
146. C. A. Richards, *The Glass Researcher* **11**, 18 (2002).
147. C. R. Kurkjian, *The Glass Researcher* **11**, 1 (2002).
148. D. E. Day, Z. Wu, C. S. Ray, and P. Hrma, *J. Non-Cryst. Solids* **241**, 1 (1998).

149. M. Karabulut, E. Melnik, R. Stefan, G. K. Marasingle, C. S. Ray, C. R. Kurkjian, and D. E. Day, *J. Non-Cryst. Solids* **288**, 8 (2001).
150. R. E. Mould, in L. J. Bonis, J. J. Duga, and J. J. Gilman, eds., *Fundamental Phenomena in the Materials Sciences*, 1967, p. 119–149.
151. D. R. Uhlmann and N. J. Kreidl, *Glass Science and Technology: Elasticity and Strength*, Academic Press, San Diego, 1980.
152. V. M. Sglavo, L. Larents, and D. J. Green, *J. Am. Ceram. Soc.* **84**, 1827 (2001); **84**, 1832 (2001).
153. A. K. Varshneya and V. Tyagi, *J. Non-Cryst. Solids* **238**, 186 (2001).
154. N. J. Kreidl and A. Angell, in D. R. Uhlmann, and N. J. Kreidl, eds., *Glass: Science and Technology*, Vol. 1, Academic Press, Boston, Mass., 1983, p. 49.
155. F. V. Tooley, *The Handbook of Glass Manufacture*, Books for the Industry, New York, 1974.
156. S. R. Scholes, *Modern Glass Practice*, Cahnners Publishings Co., 1975.
157. J. B. Wachtman, ed., in *Ceramic Innovations in the 20th Century*, The American Ceramic Society, Westerville, Ohio, 1999.
158. <http://www.oit.doe.gov/glass/pdfs/glass2002profile.pdf>; Energy and Environmental Profile of the U. S. Glass Industry, US DOE/OIT, April 2002.
159. Refractories, The Refractories Institute, Pittsburgh, Pa. 1998, p. 33.
160. Praxair Integrated Batch and Cullet Preheater System: <http://www.oit.doe.gov/glass/factsheets/cullet.pdf>.
161. M. J. Damsell, M. L. Joshi, J. R. Latter, and D. B. Wishnick, *Glass Technol.* **37**, 114 (1996).
162. E. R. Begley, *Guide to Refractory and Glass Reactions*, Cahnners, Boston, 1970.
163. M. Velez, M. Karakus, and R. E. Moore, *Ceram. Industry(Suppl.)* GMT 6 (Sept. 1998).
164. A. Gupta and D. Clendenen, *Am. Ceram. Soc. Bull.* **81**, 57 (2002).
165. *ASTM C24 Standard Test Method for Pyrometric Cone Equivalent (PCE) of Fireclay and High Alumina Refractories*.
166. M. Velez, J. M. Almanza, and M. Karakus, *Am. Ceram. Soc. Bull.* **80**(9), 33 (2001).
167. M. Velez, M. Karakus, R. E. Moore, *Refractories Appl. News* **7**(6), 32 (2002).
168. M. Velez, T. Huang, M. Karakus, W. L. Headrick, and R. E. Moore, *Taikabutsu Overseas (Jpn.)* **23**(1), 2003.
169. M. Velez, M. Karakus, W. L. Headrick, R. E. Moore, and S. L. Cabral da Silva, *Am. Ceram. Soc. Bull.* **81**(10), 46 (2002).
170. M. Velez, *Refractories Appl.* **6**(1), 14 (2001).
171. [http://www.udri.udayton.edu/udri\\_extranet/dlcm/home.asp](http://www.udri.udayton.edu/udri_extranet/dlcm/home.asp).
172. <http://www.ctcms.nist.gov/php/oof/index.html>
173. *DOE OIT portfolio 2002*: <http://www.oit.doe.gov/glass/portfolio.shtml>
174. “Sensors for Glassmaking”, *The Glass Researcher* **8**(2), 1 (1999); Part II, **10**(1) 1 (2000).
175. O. Claussen and C. Russel, *Glastech. Ber./Glass Sci. Technol.* **70**(8), 231 (1997).
176. K. D. Sienerth and H. D. Schreiber, *The Glass Researcher* **8**(2), 10 (1999).
177. R. Cook, R. Arunkumar, and O. P. Norton, *Glass Res.* **10**(1), 8 (2000).
178. S. G. Buckley, P. M. Walsh, D. H. Hahn, R. J. Gallagher, M. K. Misra, J. T. Brown, S. S. C. Tong, F. Quan, K. Bhatia, K. K. Koram, V. I. Henry, and R. D. Moore, in *Proc. 60th Conference on Glass Problems*, The American Ceramic Society, 2000, p. 183.
179. S. S. Tong, J. T. Brown, and L. H. Kotacska, *Ceram. Eng. Sci. Proc.* **18**(1), 208 (1997).
180. J. M. Almanza, “Development of a High Temperature NaOH Vapor Sensor Based on a Beta-alumina Cell,” Ph.D. dissertation, University of Missouri-Rolla, March 2003.
181. S. F. Rice, M. D. Allendorf, M. Velez, J. M. Almanza, and T. Burns, “Laser-Based Sensor for Measuring NaOH and KOH in Furnaces,” presented at the Annual Meeting (104th) American Ceramic Society., St. Louis, Mo., April 28–May 1, 2002.

182. P. Walsh, *Glass Res.* **10**(1), 3 (2000); <http://www.oit.doe.gov/glass/factsheets/monitoringalkali.pdf>
183. S. M. Pilgrim, *The Glass Researcher* **8**(2), 20 (1999).
184. R. E. Dutton and D. A. Stubbs, "An Ultrasonic Sensor for High Temperature Materials," in S. Viswanathan, R. G. Reddy, and J. C. Malas, eds., *Sensors and Modeling in Materials Processing: Techniques and Applications*, The Minerals, Metals & Materials Society, 1997, pp. 295–303.
185. J. R. Sebastian; University of Dayton Research Institute; <http://www.oit.doe.gov/cfm/fullarticle.cfm/id=658>
186. M. J. Sansalone and W. B. Street, *Impact-Echo: Nondestructive Evaluation of Concrete and Masonry*, Bullbrier Press, Ithaca, N.Y., 1997.
187. Physical Acoustics Corporation, <http://www.impact-echo.com/Impact-Echo/impact.htm>
188. B. J. Jaeger, "Refractory Wall Thickness Measurements in High Temperature Environments and in Thermal and Material Property Gradients Using the Impact-Echo Method," Ph.D. dissertation, Cornell University, 2000.
189. R. Zoughi; University of Missouri-Rolla, <http://www.oit.doe.gov/cfm/fullarticle.cfm/id=658>
190. R. Zoughi, L. K. Wu, and R. K. Moore, *Microwave J.* **28**(11), 183 (1985).
191. H. J. Muller-Simon and K. W. Mergler, *Glastech. Ber.* **61**(10), 293 (1988).
192. A. J. Faber, R. Bauer, J. Plessers, and T. Tonthat, in *Fundamentals of Glass Science and Technology*, 4th ESG Conference, Vaxjo, Sweden, 1997, p. 282.
193. W. Von Drasek, *Ceram. Eng. Sci. Proc.* **19**(1), 29 (1998).
194. S. Keyvan; University of Missouri-Columbia; [http://www.oit.doe.gov/sens\\_cont/factsheets/flame.pdf](http://www.oit.doe.gov/sens_cont/factsheets/flame.pdf)
195. A. J. Faber, *Glastech. Ber.* **64**(5), 17 (1991).
196. A. J. Faber, *The Glass Researcher* **8**(2), 4 (1999).
197. K. Hoger and G. H. Frischat, *Ceram. Trans.* **29**, 55 (1993).
198. R. F. Conti, G. A. Pecoraro, and T. A. Cleary, *Glass Res.* **8**(2), 14 (1999).
199. N. M. Carlson, Idaho National Engineering and Environmental Laboratory; <http://www.inel.gov/featuresstories/2-99hightemp.shtml>
200. P. Woskov (ppw@psfc.mit.edu), Plasma Science & Fusion Center Massachusetts Institute of Technology: <http://www.psfc.mit.edu/plasmatech/milliwave.html>
201. M. K. Choudhary, *Glass Res.* **6**(2), 7 (1997).
202. TNO Institute of Applied Physics, Eindhoven, The Netherlands. [http://www.tpd.tno.nl/TPD/pdfdocs/fsp\\_papr1057.pdf](http://www.tpd.tno.nl/TPD/pdfdocs/fsp_papr1057.pdf)
203. Glass Service Ltd., Vsetin, Czech Republic. <http://www.gsl.cz/consultation.htm>
204. M. G. Carvalho, Mechanical Engineering Dept., Instituto Superior Tecnico/Technical University of Lisbon, Lisbon, Portugal. <http://www.dem.ist.utl.pt/DEM/>
205. DOE/OIT R&D Portfolio: <http://www.oit.doe.gov/glass/factsheets/spaceglass.pdf>; Development and Validation of a Coupled Combustion Space/Glass Bath Furnace Simulation at Argonne National Laboratory.
206. D. E. Day, *The Glass Researcher* **4**, 5 (1995).
207. L. Klein, *Sol-Gel Technology for Thin Films, Fibers, Preforms, Electronics, and Specialty Shapes*, Noyes Publications, Park Ridge, N.J., 1988.
208. C. J. Brinker and G. W. Scherer, *Sol-gel Science: the Physics and Chemistry of Sol-Gel Processing*, Academic Press, Boston, 1990.
209. A. Sarkar, F. Kirkbir, and S. Raychaudhuri, *Key Eng. Mater.* **150**, 153 (1998).
210. C. H. Winter and D. M. Hoffman, eds., *Inorganic Materials Synthesis: New Directions for Advanced Materials*, Washington, D.C., American Chemical Society, Oxford University Press, 1999.
211. S. R. Kaluri, R. S. Howell, and D. W. Hess, "Helical Resonator Plasma Oxidation of Amorphous and Polycrystalline Silicon for Flat Panel Displays", in, M. K. Hatalis,

- ed., *Flat panel display materials II: symposium held April 8–12, 1996, San Francisco, Calif.*, Materials Research Society, Pittsburgh, Pa., 1997.
212. P. C. Schultz, "Vapor Phase Materials and Processes for Glasses Optical Waveguides", in *Fiber Optics Advances in Research and Development*, Plenum Press, New York, 1979.
213. G. W. Scherer and P. C. Schultz, "Unusual Methods of Making Glass," in N. J. Kreidl and D. R. Uhlmann, eds., *Glass: Science and Technology*, Vol. III, Academic Press, New York, 1979.
214. K. Hirao, *Ceram. Jpn.* **36**, 652 (2001).
215. I. M. Reaney, T. Maeder, K. G. Brooks, and P. Mural, "Microstructural Characterization of Pb (Zr,Ti)O<sub>3</sub> Thin Films Deposited by In-situ Reactive Sputtering," p. 219, in W. E. Lee, ed., *Ceramic Films and Coatings*, Institute of Materials, London, 1995.
216. J. W. Diggle, in J. W. Diggle, ed., *Oxides and Oxide Films*, Marcel Dekker, New York, 1981.
217. D. Rue, H. Abbasi, Gas Technology Institute; [http://griweb.gastechnology.org/pub/abstracts/gri90\\_0062.html](http://griweb.gastechnology.org/pub/abstracts/gri90_0062.html)
218. J. LeBlanc, R. Marshall, G. Prusia, T. Clayton, N. Simpson, and A. Richardson, *Ceramic Ind.* **152**, 42 (2002).
219. U. S. Pat. 6,237,369 (May 29, 2001), J. R. LeBlanc, A. Khalil, M. Rifat, D. J. Baker, H. P. Adams, and J. K. Hayward; (to Owens Corning Fiberglas Technology, Inc. and The BOC Group, Inc.).
220. Milan Hajek, [hajek@icpf.cas.cz](mailto:hajek@icpf.cas.cz); Institute of Chemical Process Fundamentals AS CR, Rozvojova 135, 165 02 Prague 6-Suchdol, Czech Republic; <http://www.microwave-glass.com/>.
221. <http://fire.relarn.ru/lab219/uste2.htm>
222. <http://www.vniitvch.spb.ru/english/indheat/oxide2.htm>
223. A. C. Deneys and D. G. C. Robertson, Flow Visualization and Temperature Measurements Close to the Arc Attachment Zone of a Laboratory Scale DC Arc Furnace for Slag Cleaning, in N. El-Kaddah, ed., *Fluid Flow Phenomena in Metals Processing*, The Metallurgical Society, Warrendale, Pa. 1999, pp. 127.
224. Mitsubishi Fluidized Bed incinerator; [http://nett21.unep.or.jp/CTT\\_DATA/WASTE/WASTE\\_3/html/Waste-086.html](http://nett21.unep.or.jp/CTT_DATA/WASTE/WASTE_3/html/Waste-086.html)
225. US DOE Glass Manufacturing Industry Council: <http://www.gmic.org/pubs.html>
226. U.S. Pat. 4,738,938 (Apr. 19, 1988), G. E. Kunkle, W. M. Welton, and R. L. Schwenninger (to PPG Industries, Inc.).
227. H. E. Nystrom and P. B. Thompson, *Refractories Appl.* **3**, 5 (1998).
228. V. L. Block, ed., *The Use of Glass in Buildings*, ASTM International, West Conshocken, Pa.
229. West Valley Nuclear Services: <http://www.wvnsco.com>
230. N. J. Kreidl, *J. Non-Cryst. Solids* **123**, 377 (1990).
231. J. E. Shackelford, ed., *Bioceramics: Applications of Ceramic and Glass Materials in Medicine*, Uetikon-Zurich, Switzerland; Trans Tech Publications Ltd., Enfield, N.H., 1999.
232. T. Abraham, ed., *Advanced Glasses and Glass Ceramics: Materials, Processing, New Developments, Applications, and Markets*, Business Communications Co., 1996; <http://www.buscom.com/advmat/GB094R.html>
233. P. W. L. Graham, *The Glass Researcher* **1**(2), 4 (1991).
234. D. R. Hartman, *The Glass Researcher* **4**(2), 6 (1995).
235. W. C. LaCourse, *The Glass Researcher* **1**(2), 1 (1991).
236. <http://www.o-i.com/about/corporate/patents.asp>
237. PPG Corporation Products and Services web site: <http://corporate.ppg.com/PPG/Corporate/AboutUs/ProductsandServices/documents/P%20&%20S%20brochure%202002%20final.pdf>

238. U.S. Pat. 6,416,827 (July 9, 2002), S. Chakrapani, S. M. Slovak, R. L. Saxe, and B. Fanning (to Research Frontiers Inc.); <http://www.spd-systems.com/photogallery.htm>
239. U.S. Pat. 6,027,766 (July 23, 1997) C. B. Greenberg, C. S. Harris, V. Korthuis, C. A. Kutilek, D. E. Singleton, J. Szanyi, and J. P. Thiel, (to PPG Industries).
240. D. S. Ginley and C. Bright, *MRS Bull.* **25**(8), 15 (2000).
241. L. L. Hench and J. Wilson, eds., *An Introduction to Bioceramics*, World Scientific, Singapore, 1993.
242. L. L. Hench, *Biomaterials* **19**, 1419 (1998).
243. W. Cao and L. L. Hench, *Ceramics Int.* **22**, 493 (1996).
244. L. L. Hench and J. K. West, *Life Chem. Rep.* **13**, 187 (1996).
245. H. Oonishi, S. Kushitani, E. Yasukawa, H. Iwaki, L. L. Hench, J. Wilson, E. Tsuji, and T. Sugihara, *J. Clin. Orthop. Related Res.* **334**, 316 (1997).
246. I. D. Xynos, M. V. J. Hukkanen, J. J. Batten, L. D. Buttery, L. L. Hench, and J. M. Polak, *Calcif. Tissue Int.* **67**, 321 (2000).
247. F. Baldini and A. G. Mignani, *MRS Bull.* **27**(5), 383 (2002).
248. D. E. Day, *Glass Res.* **4**, 5 (1995); <http://www.mo-scicorp.thomasregister.com/olc/mo-scicorp/>.
249. W. J. Tomlinson, *Appl. Opt.* **19**, 1127 (1980).
250. D. S. Kindred, J. Bentley, and D. T. Moore, *Appl. Opt.* **29**, 4036 (1990).
251. B. G. Potter and J. H. Simmons, *Phys. Rev.* **B37**, 10838 (1988).
252. P. Horan and W. Blau, *Z. Phys.* **D12**, 501 (1989).
253. W. Chen, S. Wang, J. Cheng, and Z. Liang, *J. Chin. Ceram. Soc.* **26**(3), 351 (1998).
254. N. Hiroyuki and J. D. Mackenzie, *Optical Eng.* **26**, 102 (1987).
255. C. Lopez, K. A. Richardson, M. de Castro, S. Seal, D. K. Verma, A. Shulte, C. Rivero, A. Villeneuve, T. V. Gastian, K. Turcotte, A. Saliminia, and J. Laniel, *J. Am. Ceram. Soc.* **85**(6), 1372 (2002).
256. J. D. Mackenzie, *J. Non-Cryst. Solids* **48**, 1 (1982).
257. K. T. V. Grattan and T. Sun, *MRS Bull.* **27**(5), 389 (2002).
258. P. Ferdinand, S. Magne, V. Dewynter-Marty, S. Rougeault, and L. Maurin, *MRS Bull.* **27**(5), 400 (2002).
259. B. G. Potter, K. Simmons-Potter, and T. D. Dunbar, *J. Non-Cryst. Solids* **277**(2–3), 114 (2000).
260. <http://www.llnl.gov/nif>
261. C. Jantzen, N. Bibber, D. Beam, C. Crawford, and M. Picketed, *Ceram. Trans.* **39**, 313 (1994).
262. D. Kim, P. Hamma, D. Lamar, and M. Elliot, *Ceram. Trans.* **45**, 39 (1995).
263. W. Rankin, "Advances in Ceramics", in *Nuclear Waste Management I*, Vol. 8, American Ceramic Society, Westerville, Ohio, 1980, pp. 559–566.
264. F. Lifanov, S. Stefanovsky, A. Kobelev, A. Savkin, O. Knyazev, T. Lashchenova, S. Merlin, and P. Roux, "Vitrification of Simulated Intermediate-Level French and Russian Waste in Cold Crucible Based Plant," in *Material Research Society Symposium Proceedings*, Vol. 412, Materials Research Society, Westerville, Ohio, 1996, pp. 163–171.
265. D. Bennert, T. Overcamp, D. Bickford, C. Jantzen, and C. Cicero, *Ceram. Trans.* **45**, 73 (1995).
266. F. Chen and D. E. Day, *Ceram. Trans.* **93**, 213 (1999).
267. U.S. Pat. 5,840,638 (Nov. 24, 1998), H. Cao, J. W. Adams and P. D. Kalb (to Brookhaven Science Associates).
268. J. C. Marra, T. J. Overcamp, and D. L. Erich, *Ceram. Trans.* **41**, 241 (1996).
269. H. Matzke and E. Vernaz, *J. Nucl. Mater.* **201**, 295 (1993).
270. G. K. Marasinghe, M. Karabulut, C. S. Ray, and D. E. Day, *J. Non-Cryst. Solids* **263–264**, 146 (2000).

271. S. T. Reis, M. Karabulut, and D. E. Day, *J. Nucl. Mater.* **304**, 87 (2002).
272. M. Karabulut, G. K. Marasinghe, P. G. Allen, C. H. Booth, and M. Grimsditch, *J Mater. Res.* **15**, 1972 (2000).
273. M. G. Mesko and D. E. Day, *J. Non-Cryst. Solids* **273**, 27 (1999).
274. D. E. Day, Z. Wu, C. S. Ray, and P. Hrma, *J. Non-Cryst. Solids* **241**, 1 (1998).
275. S. T. Reis, M. Karabulut, and D. E. Day, *J. Non-Cryst. Solids* **292**, 150 (2001).
276. M. G. Mesko, D. E. Day, and B. C. Bunker, in W. W. Schulz and N. J. Lombardo, eds., *Science and Technology for Disposal of Radioactive Tank Wastes*, Plenum Press, New York, 1998.
277. Freedomia Group Market Research: <http://www.fredoniagroup.com/construction.html>

DAVID C. BOYD  
PAUL S. DANIELSON  
DAVID A. THOMPSON  
Corning Incorporated  
MARIANO VELEZ  
SIGNO T. REIS  
RICHARD K. BROW  
University of Missouri-Rolla